American Mineralogist, Volume 90, pages 969–983, 2005

Crystal chemistry of Zn-rich rhodonite ("fowlerite")

WENDY R. NELSON AND DANA T. GRIFFEN*

Department of Geology, Brigham Young University, Provo, Utah 84602, U.S.A.

ABSTRACT

Rhodonite (ideally $MnSiO_3$) is a triclinic pyroxenoid that typically contains significant concentrations of Ca, Fe, and Mg. A variety called fowlerite contains concentrations of Zn up to 10 wt% and has been found only at Franklin, New Jersey. Data from electron microprobe analyses, single-crystal X-ray structure refinements, and preliminary Mössbauer spectra suggest marked differences in the crystal chemistry of rhodonite and fowlerite. Cations in Zn-poor rhodonites and in fowlerites exhibit distinct substitutional trends. Substitution of Zn in fowlerite occurs entirely at M4, and Ca displays a stronger preference for M5 in fowlerite than in Zn-poor rhodonite. Further, the distinctive compositional variations in fowlerite lead to strongly mutually correlated lattice parameter variations distinct from those in Zn-poor rhodonite. Mean M-O distances in fowlerite, with the exception of <M2-O>, are strongly correlated with all unit-cell edges. For Zn-poor rhodonites, neither <M2-O> nor <M4-O> are significantly correlated with cell edges, and the mean bond lengths for M1, M3, and M5 are correlated strongly with only *a* and *b*.

The most striking distinctions between fowlerite and typical rhodonite occur in the geometrical details of M4 and M5. Distortion in the M4 site of magnesian rhodonite, typical Mn-rich rhodonite, and fowlerite increases with both increasing electron population and mean electronegativity. The M4 site assumes increasing amounts of tetrahedral character with increasing electron density (i.e., increasing Zn concentration). As M4 becomes more Zn-rich, tetrahedral, and covalent in character, M5 becomes more Ca-rich, less distorted, and more ionic in character. This suggests that "pure" fowlerite (nominally $Ca_{0.2}Zn_{0.2}Mn_{0.6}O_3$, or $CaZnMn_3O_{15}$) may contain an unequivocally four-coordinated M4 site occupied solely by Zn, and with Ca largely restricted to M5.

INTRODUCTION

Rhodonite is the Mn-rich member of the pyroxenoid group, and, like all pyroxenoids, it is triclinic. Although the conventional space group $P\bar{1}$ was originally used in characterizing the unit cell, the unconventional space group $C\bar{1}$ now used makes comparisons with pyroxenes and other pyroxenoids more intuitive (Ohashi and Finger 1975). The rhodonite structure (Fig. 1), solved by Liebau et al. (1959) and redetermined and refined by Peacor and Niizeki (1963), contains silicate chains made up of repeating five tetrahedron units—the fünferketten of Liebau (1959). These silicate chains extend along **c** and are stacked with tetrahedra alternately pointing along reciprocal lattice vectors +**a*** and –**a*** in (100) layers, in a manner analogous to pyroxenes. As in pyroxenes, juxtaposed tetrahedral chains define M sites in which metals reside. Rhodonite contains five crystallographically distinct M sites, designated M1 through M5. M1, M2, and M3 are six-coordinated, M5 is seven-coordinated, and the coordination number of M4 is examined in detail in this paper.

The ideal chemical formula of rhodonite is often written $MnSiO_3$. Rhodonite of this composition has been synthesized (Ito 1972), but has not been reported to occur naturally. A more realistic ideal formula is the one used by Liebau et al. (1959), $(Mn,Ca)SiO_3$, but Fe and Mg are common minor substituents. A Zn-rich variety, occurring at Franklin, New Jersey, was initially described by Torrey (1822), although he misidentified it as "manganesian feldspar." It was given the name "fowlerite" in 1825 in honor of Samuel Fowler (Shepard 1832). With the recognition that "fowlerite" is a Zn-rich variety of rhodonite (e.g., Camac 1852), its treatment as a distinct mineral species was eventually discontinued. To date, Franklin, New Jersey, is the only locality from which rhodonite containing substantial Zn has been reported. The recognized variety "fowlerite" is commonly cited as containing up to 10 wt% ZnO (e.g., Roberts et al. 1992).

Various workers have studied crystal chemical aspects of typical rhodonite (i.e., those containing only Fe and Mg as significant substituents for the major cations Mn and Ca), either as a primary focus or as related to other pyroxenoids. These studies include Peacor and Niizeki (1963), Momoi (1964), Ito (1972), Ohashi and Finger (1975), Viswanathan and Harneit (1986), Pinckney and Burnham (1988), and Livi and Veblen (1992). Sapountzis and Christofides (1982) described a Ca-poor rhodonite, and Peacor et al. (1978) refined the crystal structure of an Mg-rich rhodonite. Dickson (1975) presented Mössbauer spectra of rhodonite. Except for brief mention of some effects of Zn on lattice parameters (Viswanathan and Harneit 1986) there has been no systematic investigation of Zn-rich rhodonite (fowlerite) to date. We present here such a study.

To avoid ambiguity and the need for repetitive explanation, we consistently use the term "rhodonite" hereafter to indicate the typical Zn-poor pyroxenoid and the term "fowlerite" to refer to Zn-rich "rhodonite," although we show that the relationship between the two is more complex than has heretofore been recognized.

* E-mail: dana_griffen@byu.edu

0003-004X/05/0506–969$05.00/DOI: 10.2138/am.2005.1694

Experimental methods and results

Electron microprobe

Microprobe analyses were performed with a Cameca SX-50 electron probe microanalyzer operated at 15 kV excitation voltage and 20 nA beam current. Specimens, consisting of polished grain mounts, were analyzed for Si, Al, Mg, Ca, Ti, Mn, Fe, and Zn. Well-analyzed silicates were used as standards for all elements except Zn, for which Zn metal was the most suitable standard available. Data were reduced to oxide weight percents using the PAP correction procedure (Pouchou and Pichoir 1985). The results are presented in Table 1. Neither Ti nor Al was detected in concentrations exceeding 0.003 apfu based on a chemical formula containing three oxygen atoms. Table 1 shows that eleven of the 19 specimens analyzed are typical (i.e., Zn-poor) rhodonite and eight are fowlerite.

Single crystal X-ray diffraction and crystal structure refinement

Crystal structure refinements were carried out for the eight rhodonite and eight fowlerite specimens from which suitable single crystals could be extracted. X-ray intensities were collected with an Enraf Nonius CAD4 Mach automated single-crystal X-ray diffractometer equipped with a graphite monochromator and using Mo$K\alpha$ radiation. For each crystal, data were collected to 65° 2θ ($\sin\theta/\lambda$ = 0.76) using ω-2θ scans at scan rates dependent upon intensities. Three standard reflections were measured every 200 reflections. Precise unit-cell parameters were determined from high angle reflections (θ > 20°) that were automatically centered following data collection. In addition, psi scans were collected for seven reflections

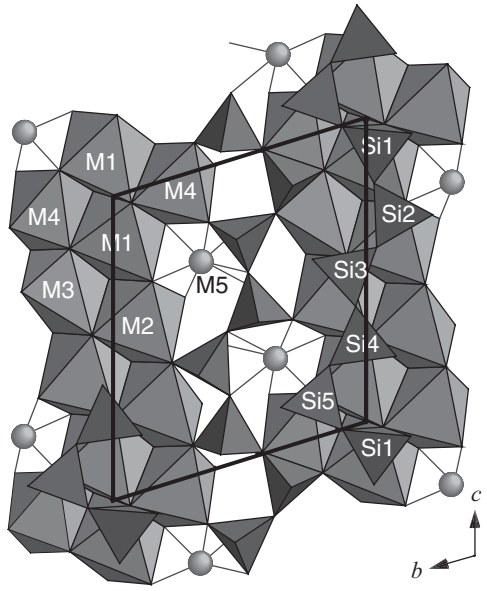

Figure 1. The (100) projection of the crystal structure of rhodonite.

Table 1. Electron microprobe analyses of specimens used in this study

Specimen	15-4013	15-4018	15-4019	15-4024	15-4025	15-4026	15-4030	15-4031	15-3032	
Locality	Unspecified	Pajsberge, Sweden	Unspecified	Cumberland, Rhode Island	Plainfield, Maine	Plainfield, Maine	Huanuco, Peru Peru	Huanuco, U.S.A.	New York,	
SiO_2	45.91	46.15	46.02	45.59	45.69	46.28	46.28	46.26	45.71	
TiO_2	0.02	0.01	0.02	0.00	0.01	0.00	0.00	0.01	0.01	
Al_2O_3	0.01	0.01	0.01	0.01	0.01	0.01	0.12	0.09	0.01	
MgO	0.25	1.03	0.22	0.60	0.08	0.39	1.33	1.42	0.13	
FeO	6.54	2.12	2.44	4.40	1.93	3.40	1.11	0.68	12.34	
MnO	45.07	43.68	48.04	45.94	48.13	46.35	44.33	44.91	40.21	
ZnO	0.02	0.13	0.03	0.08	0.03	0.05	0.03	0.04	0.16	
CaO	2.62	6.09	3.51	2.57	3.65	3.80	6.33	6.28	1.73	
Total	100.44	99.22	100.29	99.19	99.53	100.28	99.53	99.69	100.30	
Cations based on 3 oxygen atoms pfu										
Si	0.993	0.994	0.994	0.995	0.994	0.996	0.992	0.990	0.994	
Ti	0.000	0.000	0.000	0.000	0.000	0.000	0.000	0.000	0.000	
Al	0.000	0.000	0.000	0.000	0.000	0.000	0.003	0.002	0.000	
Mn	0.826	0.797	0.879	0.849	0.887	0.845	0.804	0.814	0.740	
Fe	0.118	0.038	0.044	0.080	0.035	0.061	0.020	0.012	0.224	
Mg	0.008	0.033	0.007	0.020	0.003	0.013	0.042	0.045	0.004	
Zn	0.000	0.002	0.000	0.001	0.000	0.001	0.000	0.001	0.003	
Ca	0.061	0.141	0.081	0.060	0.085	0.088	0.145	0.144	0.040	

Specimen	15-3033	15-4034	15-4006	15-4014	15-4020	15-4027	15-4028	15-4029	15-4040	15-4041
Locality	Broken Hill, Australia	Broken Hill, Australia	Franklin, New Jersey	Unspecified	Unspecified	Franklin, New Jersey	Franklin, New Jersey	Franklin, New Jersey	Franklin, New Jersey	Franklin, New Jersey
SiO_2	45.94	45.83	46.35	46.26	46.69	45.95	46.46	46.75	46.70	46.52
TiO_2	0.02	0.02	0.04	0.00	0.02	0.01	0.00	0.02	0.01	0.02
Al_2O_3	0.03	0.04	0.01	0.08	0.04	0.02	0.02	0.01	0.03	0.02
MgO	0.30	0.25	1.54	1.51	1.00	1.93	0.88	0.83	0.85	0.86
FeO	11.76	11.92	2.79	3.01	1.66	0.82	1.91	2.35	1.48	0.00
MnO	37.35	37.91	35.71	35.15	35.92	37.94	38.04	36.30	37.99	37.86
ZnO	0.33	0.35	6.96	7.22	6.04	6.64	5.09	5.22	5.32	5.67
CaO	4.32	3.94	6.59	6.70	8.61	5.69	7.61	8.75	7.82	9.04
Total	100.05	100.26	99.99	99.93	99.98	99.00	100.01	100.23	100.20	99.99
Cations based on 3 oxygen atoms pfu										
Si	0.993	0.991	0.994	0.993	0.997	0.994	0.996	0.997	0.997	0.995
Ti	0.000	0.000	0.001	0.000	0.000	0.000	0.000	0.000	0.000	0.000
Al	0.001	0.001	0.000	0.002	0.001	0.001	0.001	0.000	0.001	0.001
Mn	0.684	0.694	0.649	0.639	0.650	0.695	0.690	0.655	0.687	0.686
Fe	0.213	0.216	0.050	0.054	0.030	0.015	0.034	0.042	0.026	0.000
Mg	0.010	0.008	0.049	0.048	0.032	0.062	0.028	0.026	0.027	0.027
Zn	0.005	0.006	0.110	0.114	0.095	0.106	0.081	0.082	0.084	0.090
Ca	0.100	0.091	0.151	0.154	0.197	0.132	0.175	0.200	0.179	0.207

in each data set to facilitate empirical absorption corrections.

Raw intensity data were reduced to structure amplitudes and an empirical absorption correction was applied according to the method of North et al. (1968) using the WinGX suite of programs (Farrugia 1999). The threshold expression $I > 2\sigma(I)$ was used only in the calculation of residuals and was not used to limit the choice of reflections for refinement. We used the final refined atomic positions of Peacor et al. (1978) as initial atomic positions. Atomic scattering factors for Mn^{2+}, Si, O^{-}, and Ca^{2+} were taken from Cromer and Mann (1968). Refinements were carried out with SHELX-97 (Sheldrick 1997) in the following way for all specimens: M1, M2, M3, and M4 were assigned the scattering factor of Mn^{2+}, and M5 was assigned as Ca^{2+}. After an initial least-squares cycle to estimate the overall scale factor, atomic positions were varied for three cycles, followed by variation of the positions and isotropic displacement parameters. Following successful convergence, all isotropic displacement parameters were converted to anisotropic displacement parameters. These were refined alternately with site occupancy factors for the M sites, then the scale factor, atomic positions, anisotropic displacement parameters, and M-site occupancies were varied simultaneously for three to five cycles of refinement. Examination of observed and calculated structure amplitudes revealed the need for an extinction correction in some cases, so for consistency, an extinction correction was applied to all refinements in the final cycles. Final electron-density difference maps showed no significant anomalous positive or negative peaks. Data collection and refinement parameters other than those given above are summarized in Table 2. Residuals (*R*) and weighted residuals (*wR*) are based on F^2 rather than *F*, and are thus larger than conventional *R*-factors. Observed and calculated structure amplitudes are provided in Table 3[1]. Table 4 gives refined lattice parameters. Final atomic positions, electron populations at the M sites, and equivalent isotropic displacement parameters are in Table 5. Anisotropic displacement factors are given in Table 6[1]. Tables 7 and 8 display selected interatomic distances and bond angles, respectively.

[1] For a copy of Tables 3 and 6, Document item AM-05-014, contact the Business Office of the Mineralogical Society of America (see inside front cover of recent issue) for price information. Deposit items may also be available on the *American Mineralogist* web site at http://www.minsocam.org.

DISCUSSION

Chemical interrelationships and cation site assignments

Figure 2 graphically displays differences between the chemical relationships exhibited by the specimens examined in our study, and leads to the following observations. First, there is a substantial gap between the Zn concentrations in fowlerite and rhodonite, and thus we have no evidence for solid solution between the two. Second, although there is some overlap in the distributions of the other M-site substituents, Ca and Mg contents tend to be higher, and the Fe content tends to be lower in fowlerite than in rhodonite. In addition, Mn concentrations are generally lower in fowlerite than in rhodonite. These observations suggest the possibility that somewhat different metal substitutions govern the crystal chemistry of fowlerite than that of rhodonite, and we investigate that possibility below.

The root-mean-square difference between the number of M-site electrons predicted by the microprobe analyses and the number determined by the X-ray site refinements is < 1%, with a tendency for the probe analyses to predict a slightly higher number. The maximum differences (referred to the microprobe analyses) are +1.68% and –0.97%, but this good agreement does not lead unambiguously to cation site assignments. With twice the number of unknowns (i.e., numbers of cations of each type at each M site) as the number of constraining relationships (as governed by the refined X-ray electron populations and the microprobe analyses), assignment of cations to sites admits of no unique solution.

Table 9 shows a plausible cation site assignment for a typical

TABLE 2. Crystal-structure refinement parameters

	15-4018	15-4024	15-4025	15-4026	15-4030	15-4031
R	0.036	0.047	0.05	0.062	0.053	0.048
wR	0.078	0.105	0.107	0.13	0.131	0.121
R(all)	0.079	0.093	0.124	0.143	0.089	0.073
GooF	1.015	1.03	0.992	1.114	1.042	1.087
No. refns	4083	4182	4174	4171	4202	4180
No. refns I > 2σ(I)	3003	2919	2572	2578	3097	3274
Extinction factor	0.0013(1)	0.0008(2)	0.0005(2)	0.0004(2)	0.0013(3)	0.0007(3)
R(int)	0.031	0.029	0.047	0.010	0.027	0.017
Max/min transmission	0.999/0.923	0.999/0.888	0.979/0.848	0.969/0.769	0.938/0.616	0.999/0.696
Crystal size	0.26 × 0.23 × 0.11	0.34 × 0.34 × 0.26	0.23 × 0.23 × 0.19	0.30 × 0.24 × 0.15	0.30 × 0.23 × 0.17	0.38 × 0.32 × 0.22
	15-4033	15-4034	15-4006	15-4014	15-4020	15-4027
R	0.041	0.041	0.029	0.03	0.039	0.033
w*R*	0.097	0.095	0.071	0.074	0.099	0.087
R(all)	0.078	0.087	0.043	0.045	0.061	0.047
GooF	1.1	1.02	1.112	1.083	1.031	1.07
No. refns	4017	4153	4176	4195	4152	1975
No. refns *I* > 2σ(*I*)	3104	2926	3484	3517	3266	1645
Extinction factor	0.0094(4)	0.0006(2)	0.0028(2)	0.0016(2)	0.0009(2)	0.0012(2)
R(int)	0.007	0.024	0.020	0.019	0.030	0.020
Max/min transm. fact.	0.991/0.706	0.998/0.835	0.984/0.926	0.990/0.826	0.998/0.755	0.988/0.857
Crystal size (mm)	0.18 × 0.15 × 0.08	0.26 × 0.23 × 0.15	0.30 × 0.30 × 0.11	0.34 × 0.19x0.15	0.38 × 0.30 × 0.23	0.26 × 0.26 × 0.14
	15-4028	15-4029	15-4040	15-4041		
R	0.031	0.029	0.055	0.031		
w*R*	0.078	0.072	0.142	0.077		
R(all)	0.043	0.044	0.071	0.047		
GooF	1.059	1.07	1.076	1.079		
No. refns	4180	4165	4205	4166		
No. refns *I* > 2σ(*I*)	3551	3488	3476	3496		
Extinction factor	0.0037(2)	0.0046(2)	0.0048(5)	0.0065(3)		
R(int)	0.027	0.017	0.021	0.021		
Max/min transm. fact.	0.999/0.870	0.999/0.887	0.998/0.602	0.996/0.701		
Crystal size (mm)	0.26 × 0.23 × 0.19	0.36 × 0.28 × 0.17	0.41 × 0.26 × 0.23	0.30 × 0.26 × 0.15		

TABLE 4. Lattice parameters (cell edges in angstroms, angles in degrees, volumes in Å^3) of specimens used in this study

Specimen	15-4018	15-4024	15-4025	15-4026	15-4030	15-4031
a	9.8381(4)	9.7718(9)	9.7999(11)	9.7902(24)	9.8451(7)	9.8121(11)
b	10.5361(4)	10.5084(13)	10.5176(19)	10.5184(24)	10.5389(7)	10.5187(11)
c	12.2381(4)	12.2256(8)	12.2365(19)	12.2230(36)	12.2414(8)	12.2180(18)
α	108.697(3)	108.606(8)	108.587(14)	108.644(24)	108.692(6)	108.651(12)
β	103.335(2)	103.017(6)	103.185(12)	103.159(24)	103.299(6)	103.217(11)
γ	82.191(3)	82.482(9)	82.320(12)	82.308(20)	82.184(6)	82.308(9)
V	1166.56(8)					
Specimen	15-4033	15-4034	15-4006	15-4014	15-4020	15-4027
a	9.7834(2)	9.7648(9)	9.8456(2)	9.8768(3)	9.8393(9)	9.8337(3)
b	10.5023(2)	10.4912(9)	10.4992(2)	10.5222(3)	10.4941(9)	10.4987(3)
c	12.2338(4)	12.2228(11)	12.2005(4)	12.2180(4)	12.1977(13)	12.1966(5)
α	108.682(3)	108.671(8)	108.726(3)	108.748(3)	108.751(9)	108.699(3)
β	103.273(3)	103.177(8)	103.724(3)	103.781(3)	103.751(9)	103.597(3)
γ	82.213(2)	82.284(6)	82.113(2)	82.037(2)	82.091(9)	82.221(2)
Specimen	15-4028	15-4029	15-4040	15-4041		
a	9.8640(7)	9.8793(2)	9.8719(4)	9.8905(3)		
b	10.5237(4)	10.5298(2)	10.5262(4)	10.5423(3)		
c	12.2180(9)	12.2257(4)	12.2214(5)	12.2294(4)		
α	108.727(6)	108.744(3)	108.743(4)	108.739(3)		
β	103.705(5)	103.752(3)	103.728(4)	103.773(3)		
γ	82.082(6)	82.030(2)	82.049(3)	82.050(2)		

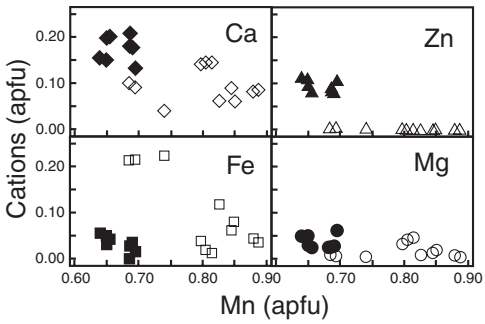

FIGURE 2. Some chemical relationships among M-site cations in rhodonite (open symbols) and fowlerite (filled symbols).

fowlerite sample (15-4029) based on the microprobe and X-ray results. The dual requirements that M4 host a large electron population (as shown by the X-ray site refinements for fowlerite) and that its site occupancy not exceed unity strongly imply that all Zn is at M4. Because the site refinement of Peacor et al. (1978) required essentially all Mg in their rhodonite to occupy M4, we have also assigned all Mg to that site. Our preliminary Mössbauer spectra (work in progress) reveal that Fe is present in all five M sites of fowlerite specimens so far investigated with this technique, so we have distributed it essentially uniformly over all five sites as a preliminary approximation. The presence of some Fe at M1, M2, and M3 requires that some Ca replace Mn at those sites, to reduce the number of electrons while keeping the atom population near unity. The displaced Mn enters M5, which is also required to raise the occupancy in that site to approximately 1 atom. In summary, for fowlerite there seems to be Mn at all sites (if there is insufficient Zn + Mg to fill M4), Fe apparently occupies all M sites (although not necessarily equally), and these distributions require that minor Ca be found at M1, M2, and M3. The geometry of M4 in fowlerite makes that site an unlikely one for Ca (discussed below).

A plausible cation distribution for a typical rhodonite (15-4024) is also given in Table 9, and it bears qualitative similarities to the distribution postulated for fowlerite (15-4029). The relatively low electron population at M4 implies that Mg occupies that site, as in fowlerite. We have again arbitrarily distributed Fe uniformly, with no claim that doing so represents reality. Mössbauer spectra (Dickson 1975; our work in progress) show Fe to be present at all five sites, however, and regardless of how it is distributed in specimen 15-4024, the distribution of Mn turns out to be much more uniform than that in specimen 15-4029 (fowlerite). Satisfying the requirements of electron population and atomic occupancy again requires Ca to be distributed over M1, M2, and M3, as well as M5. Ca is less strongly partitioned into M5 in this rhodonite than in fowlerite. Whereas some adjustments could be made to this non-unique distribution, any distribution that satisfied the X-ray site refinement, electron microprobe analysis, and preliminary Mössbauer work would have to look qualitatively much like that in Table 9.

Other workers have expressed other opinions about the location of Ca in the rhodonite structure. Peacor and Niizeki (1963), as well as Pinckney and Burnham (1988), considered Ca to occupy only M5 because of size constraints, and thus concluded that rhodonite can accommodate up to 20 mol% Ca. Observing a correlation between Ca concentration and the distortion of the M4 site, Ohashi and Finger (1975) argued that Ca may occupy both M4 and M5. Livi and Veblen (1992) concurred that most Ca occupies M5, but that some may also be at M4.

To further compare the nature of cationic substitutions in rhodonite and fowlerite, we employed principal component analysis (this statistical technique is described in, for example, Rao 1965.) For typical rhodonite, we ignored Zn because its concentration is too low for it to play an important crystal-chemical role. The first two principle components account for 96% of the variance in the data, with rotated factor loadings as shown in Table 10. We interpret the first principal component, which accounts for over half of the variance in the rhodonite compositional data, as reflecting opposite substitutional behavior of (Ca,Mg) and Fe. Because Ca and Mg are, respectively, the largest and smallest of the substituents at the M sites, we interpret these substitutions as essentially independent, with that involving Mg occurring at M4 and that involving Ca occurring at all other M sites. The

TABLE 5. Final refined fractional coordinates, electron populations, and equivalent isotropic displacement parameters (Å²)

	x	*y*	*z*	e⁻	U_{eq}
15-4018					
M1	0.00006(6)	0.03038(5)	0.14794(5)	24.9(8)	0.0069(2)
M2	0.00148(6)	0.12666(5)	0.44492(5)	24.7(8)	0.0069(2)
M3	0.01651(6)	0.20458(5)	0.72987(5)	24.7(7)	0.0068(2)
M4	0.06046(7)	0.26422(6)	0.0237(5)	23.6(8)	0.0094(2)
M5	0.99571(7)	0.35515(7)	0.30519(6)	21.7(8)	0.0121(2)
Si1	0.2046(1)	0.4507(1)	0.9110(1)		0.0050(2)
Si2	0.2123(1)	0.3669(1)	0.6539(1)		0.00482)
Si3	0.2174(1)	0.5803(1)	0.5298(1)		0.0053(2)
Si4	0.2148(1)	0.5068(1)	0.2613(1)		0.0051(2)
Si5	0.2052(1)	0.7010(1)	0.1249(1)		0.0054(2)
OA1	0.1281(3)	0.0706(2)	0.0402(2)		0.0071(4)
OA2	0.1192(3)	0.1577(3)	0.3224(2)		0.0077(5)
OA3	0.1138(3)	0.9221(3)	0.4362(2)		0.0074(5)
OA4	0.1183(3)	0.0131(3)	0.7316(2)		0.0080(5)
OA5	0.1300(3)	0.7907(2)	0.8534(2)		0.0078(5)
OA6	0.0984(3)	0.8328(2)	0.1308(2)		0.0077(5)
OB1	0.1286(3)	0.3225(3)	0.9019(2)		0.0089(5)
OB2	0.1247(3)	0.2369(2)	0.6113(2)		0.0079(5)
OB3	0.1295(3)	0.7117(3)	0.5894(2)		0.0127(5)
OB4	0.1262(3)	0.3813(3)	0.1838(2)		0.0106(5)
OC1	0.1695(3)	0.4699(2)	0.7776(2)		0.0072(4)
OC2	0.1596(3)	0.4589(3)	0.5634(2)		0.0113(5)
OC3	0.1664(3)	0.5384v	0.3869(2)		0.0086(5)
OC4	0.1585(3)	0.6422(3)	0.2201(2)		0.0078(5)
OC5	0.1465(3)	0.5930(3)	0.9956(2)		0.0077(5)
15-4024					
M1	–0.00054(7)	0.02902(7)	0.14788(6)	24.9(1)	0.0075(2)
M2	0.00095(7)	0.12814(7)	0.44549(6)	24.9(1)	0.0082(2)
M3	0.01656(7)	0.20355(7)	0.73031(6)	24.7(1)	0.0077(2)
M4	0.05979(8)	0.26466(7)	0.02610(6)	24.3(1)	0.0111(2)
M5	0.99392(9)	0.34520(8)	0.29879(7)	25.9(1)	0.0149(2)
Si1	0.2046(1)	0.4504(1)	0.9110(1)		0.0069(1)
Si2	0.2125(1)	0.3653(1)	0.6544(1)		0.0059(1)
Si3	0.2154(1)	0.5785(1)	0.5317(1)		0.0065(1)
Si4	0.2120(1)	0.5072(1)	0.2638(1)		0.0066(1)
Si5	0.2044(1)	0.7004(1)	0.1249(1)		0.0063(1)
OA1	0.1272(3)	0.0700(3)	0.0407(3)		0.0096(6)
OA2	0.1183(3)	0.1583(3)	0.3208(3)		0.0082(6)
OA3	0.1153(3)	0.9203(3)	0.4351(3)		0.0093(6)
OA4	0.1214(3)	0.0133(3)	0.7312(3)		0.0096(6)
OA5	0.1295(3)	0.7909(3)	0.8544(3)		0.0086(6)
OA6	0.099☒(3)	0.8328(3)	0.1309(3)		0.0093(6)
OB1	0.1305(4)	0.3207(3)	0.9035(3)		0.0119(6)
OB2	0.1251(3)	0.2342(3)	0.6118(3)		0.0093(6)
OB3	0.1252(3)	0.7077(4)	0.5946(3)		0.0151(7)
OB4	0.1231(4)	0.3802(3)	0.1898(3)		0.0131(7)
OC1	0.1687(4)	0.4684(3)	0.7777(3)		0.0094(6)
OC2	0.1621(4)	0.4538(4)	0.5616(3)		0.0144(7)
OC3	0.1638(4)	0.5433(4)	0.3897(3)		0.0124(6)
OC4	0.1567(3)	0.6396(3)	0.2189(3)		0.0089(6)
OC5	0.1458(3)	0.5926(3)	0.9953(3)		0.0093(6)
15-4025					
M1	–0.00034(9)	0.02954(9)	0.14809(7)	24.9(1)	0.00812(3)
M2	0.00120(8)	0.12793(9)	0.44526(7)	24.9(1)	0.00825(3)
M3	0.01663(9)	0.20381(9)	0.72996(7)	24.7(1)	0.00756(3)
M4	0.06073(10)	0.26429(9)	0.02527(7)	24.8(1)	0.01077(3)
M5	0.99431(11)	0.34853(11)	0.30080(10)	23.7(1)	0.015443)
Si1	0.2047(2)	0.4510(2)	0.9108(1)		0.0063(3)
Si2	0.2124(2)	0.3659(2)	0.6541(1)		0.0057(3)
Si3	0.2163(2)	0.5792(2)	0.5310(1)		0.0064(3)
Si4	0.2129(2)	0.5074(2)	0.2633(1)		0.0068(3)
Si5	0.2045(2)	0.7004(2)	0.1249(1)		0.0064(3)
OA1	0.1274(4)	0.0700(4)	0.0407(3)		0.0072(7)
OA2	0.1186(4)	0.1582(4)	0.3211(3)		0.0089(7)
OA3	0.1148(4)	0.9214(4)	0.4359(3)		0.0101(8)
OA4	0.1199(4)	0.0126(4)	0.7312(3)		0.0097(8)
OA5	0.1299(4)	0.7900(4)	0.8532(3)		0.0085(7)
OA6	0.0981(4)	0.8330(4)	0.1312(3)		0.0092(7)
OB1	0.1302(4)	0.3221(4)	0.9032(3)		0.0098(8)
OB2	0.1248(4)	0.2351(4)	0.6116(3)		0.0088(7)
OB3	0.1278(5)	0.7094(5)	0.5935(4)		0.0166(9)
OB4	0.1240(4)	0.3808(4)	0.1884(4)		0.0133(8)
OC1	0.1691(4)	0.4695(4)	0.7775(3)		0.0096(7)
OC2	0.1610(4)	0.4549(5)	0.5621(4)		0.0139(8)
OC3	0.1647(4)	0.5423(4)	0.3893(3)		0.0113(8)

TABLE 5.—*Continued*

	x	*y*	*z*	e⁻	U_{eq}
OC4	0.1569(4)	0.6399(4)	0.2190(3)		0.0093(7)
OC5	0.1451(4)	0.5931(4)	0.9951(3)		0.0104(8)
15-4026					
M1	–0.0003(1)	0.0295(1)	0.1479(1)	25.2(2)	0.0083(4)
M2	0.0012(1)	0.1277(1)	0.4450(1)	24.9(2)	0.0084(4)
M3	0.0167(1)	0.2039(1)	0.7302(1)	24.4(2)	0.0073(4)
M4	0.0603(1)	0.2644(1)	0.0252(1)	24.1(2)	0.0102(4)
M5	0.9944(2)	0.3483(2)	0.3008(2)	23.5(2)	0.0149(4)
Si1	0.2049(2)	0.4507(2)	0.9112(2)		0.0070(4)
Si2	0.2125(2)	0.3662(2)	0.6544(2)		0.0066(4)
Si3	0.2158(2)	0.5791(2)	0.5306(2)		0.0070(4)
Si4	0.2130(2)	0.5072(2)	0.2630(2)		0.0068(4)
Si5	0.2045(2)	0.7004(2)	0.1247(2)		0.0067(4)
OA1	0.1272(6)	0.0694(6)	0.0400(5)		0.0095(10)
OA2	0.1189(6)	0.1584(6)	0.3211(5)		0.0079(10)
OA3	0.1144(6)	0.9215(5)	0.4358(5)		0.0078(10)
OA4	0.1196(6)	0.0134(5)	0.7312(5)		0.0087(10)
OA5	0.1298(6)	0.7912(6)	0.8539(5)		0.0104(11)
OA6	0.0992(6)	0.8326(6)	0.1316(6)		0.0111(11)
OB1	0.1287(6)	0.3214(6)	0.9025(5)		0.0116(11)
OB2	0.1241(6)	0.2347(6)	0.6110(5)		0.0088(10)
OB3	0.1269(6)	0.7088(6)	0.5925(5)		0.0151(12)
OB4	0.1237(6)	0.3798(6)	0.1877(5)		0.0130(11)
OC1	0.1693(6)	0.4681(6)	0.7781(5)		0.0094(10)
OC2	0.1610(6)	0.4546(7)	0.5627(6)		0.0143(12)
OC3	0.1652(6)	0.5417(6)	0.3890(5)		0.0113(11)
OC4	0.1569(6)	0.6411(6)	0.2195(5)		0.0095(10
OC5	0.1454(6)	0.5930(6)	0.9952(5)		0.0098(10)
15-4030					
M1	0.00023(7)	0.03036(7)	0.14794(6)	24.4(1)	0.0076(2)
M2	0.00154(7)	0.12666(7)	0.44508(6)	24.5(1)	0.0079(2)
M3	0.01613(7)	0.20466(7)	0.72987(6)	24.4(1)	0.0078(2)
M4	0.05931(9)	0.26420(8)	0.02365(6)	23.3(1)	0.0107(2)
M5	0.99566(9)	0.35591(9)	0.30576(8)	21.5(1)	0.0131(3)
Si1	0.2047(1)	0.4507(1)	0.9111(1)		0.0068(2)
Si2	0.2121(1)	0.3672(1)	0.6539(1)		0.0061(2)
Si3	0.2174(1)	0.5802(1)	0.5297(1)		0.0062(2)
Si4	0.2150(1)	0.5068(1)	0.2613(1)		0.0062(2)
Si5	0.2056(1)	0.7013(1)	0.1251(1)		0.0066(2)
OA1	0.1282(3)	0.0706(3)	0.0406(3)		0.0093(6)
OA2	0.1201(3)	0.1576(3)	0.3225(3)		0.0087(6)
OA3	0.1143(3)	0.9223(3)	0.4362(3)		0.0084(6)
OA4	0.1181(3)	0.0132(3)	0.7318(3)		0.0095(6)
OA5	0.1300(3)	0.7906(3)	0.8536(3)		0.0091(6)
OA6	0.0992(3)	0.8326(3)	0.1311(3)		0.0092(6)
OB1	0.1285(4)	0.3226(3)	0.9022(3)		0.0108(6)
OB2	0.1243(4)	0.2365(3)	0.6107(3)		0.0111(6)
OB3	0.1303(4)	0.7118(3)	0.5893(3)		0.0132(7)
OB4	0.1283(4)	0.3810(4)	0.1839(3)		0.0127(6)
OC1	0.1694(3)	0.4695(3)	0.7777(3)		0.0091(6)
OC2	0.1590(3)	0.4591(4)	0.5634(3)		0.0115(6)
OC3	0.1662(3)	0.5382(3)	0.3869(3)		0.0098(6)
OC	0.1594(3)	0.6415(3)	0.2200(3)		0.0094(6)
OC5	0.1464(3)	0.5933(3)	0.9954(3)		0.0088(6)
15-4031					
M1	0.00026(6)	0.03004(6)	0.14802(5)	24.5(1)	0.0063(2)
M2	0.00127(6)	0.12716(6)	0.44510(5)	24.4(1)	0.0064(2)
M3	0.01627(6)	0.20448(6)	0.73016(5)	24.3(1)	0.0064(2)
M4	0.05944(8)	0.26430(7)	0.02431(6)	22.8(1)	0.0096(2)
M5	0.99553(8)	0.35280(8)	0.30368(7)	22.9(1)	0.0137(2)
Si1	0.2044(1)	0.4504(1)	0.9113(1)		0.0050(2)
Si2	0.2121(1)	0.3664(1)	0.6539(1)		0.0045(2)
Si3	0.2166(1)	0.5795(1)	0.5302(1)		0.0049(2)
Si4	0.2143(1)	0.5067(1)	0.2618(1)		0.0051(2)
Si5	0.2055(1)	0.7009(1)	0.1251(1)		0.0053(2)
OA1	0.1275(3)	0.0708(3)	0.0406(2)		0.0077(5)
OA2	0.1191(3)	0.1575(3)	0.3219(2)		0.0070(5)
OA3	0.1147(3)	0.9215(3)	0.4363(3)		0.0092(5)
OA4	0.1189(3)	0.0130(3)	0.7318(2)		0.0079(5)
OA5	0.1296(3)	0.7900(3)	0.8537(2)		0.0076(5)
OA6	0.0994(3)	0.8332(3)	0.1313(2)		0.0082(5)
OB1	0.1283(3)	0.3219(3)	0.9029(3)		0.0103(5)
OB2	0.1250(3)	0.2359(3)	0.6114(2)		0.0083(5)
OB3	0.1279(3)	0.7104(3)	0.5905(3)		0.0138(6)
OB4	0.1264(3)	0.3807(3)	0.1852(3)		0.0111(5)
OC1	0.1692(3)	0.4695(3)	0.7779(2)		0.0083(5)

TABLE 5.—*Continued*

	x	*y*	*z*	e⁻	U_{eq}
OC2	0.1598(3)	0.4575(3)	0.5631(3)		0.0114(5)
OC3	0.1652(3)	0.5391(3)	0.3875(2)		0.0103(5)
OC4	0.1586(3)	0.6413(3)	0.2200(2)		0.0087(5)
OC5	0.1464(3)	0.5930(3)	0.9955(2)		0.0088(5)
15-4033					
M1	–0.00085(6)	0.02972(6)	0.14763(5)	25.5(1)	0.0076(2)
M2	0.00127(6)	0.12683(6)	0.44458(5)	25.3(1)	0.0077(2)
M3	0.01677(7)	0.20350(6)	0.72977(5)	25.2(1)	0.0077(2)
M4	0.06199(8)	0.26365(7)	0.02470(6)	25.0(1)	0.0114(2)
M5	0.99470(8)	0.34929(8)	0.30121(8)	23.8(1)	0.0161(2)
Si1	0.2043(1)	0.4508(1)	0.9105(1)		0.0060(2)
Si2	0.2121(1)	0.3661(1)	0.6542(1)		0.0056(2)
Si3	0.2160(1)	0.5790(1)	0.5303(1)		0.0063(2)
Si4	0.2129(1)	0.5072(1)	0.2626(1)		0.0065(2)
Si5	0.2038(1)	0.7008(1)	0.1247(1)		0.0062(2)
OA1	0.1267(3)	0.0695(3)	0.0403(3)		0.0077(5)
OA2	0.1181(3)	0.1576(3)	0.3209(3)		0.0082(5)
OA3	0.1144(3)	0.9223(3)	0.4358(3)		0.0091(5)
OA4	0.1191(3)	0.0126(3)	0.7308(3)		0.0093(5)
OA5	0.1299(3)	0.7916(3)	0.8538(3)		0.0093(5)
OA6	0.0977(3)	0.8334(3)	0.1310(3)		0.0098(5)
OB1	0.1299(3)	0.3211(3)	0.9020(3)		0.0114(6)
OB2	0.1246(3)	0.2347(3)	0.6109(3)		0.0087(5)
OB3	0.1275(3)	0.7096(4)	0.5918(3)		0.0171(7)
OB4	0.1245(3)	0.3803(3)	0.1863(3)		0.0127(6)
OC1	0.1681(3)	0.4694(3)	0.7774(3)		0.0086(5)
OC2	0.1601(3)	0.4553(3)	0.5622(3)		0.0145(6)
OC3	0.1641(3)	0.5406(3)	0.3881(3)		0.0112(6)
OC4	0.1564(3)	0.6415(3)	0.2201(3)		0.0088(5)
OC5	0.1449(3)	0.5929(3)	0.9954(3)		0.0098(5)
15-4034					
M1	–0.00101(6)	0.02939(6)	0.14751(5)	25.4(1)	0.0077(2)
M2	0.00116(7)	0.12727(6)	0.44477(5)	25.3(1)	0.0083(2)
M3	0.01674(7)	0.20328(6)	0.72983(5)	25.0(1)	0.0073(2)
M4	0.06192(8)	0.26382(7)	0.02522(6)	25.2(1)	0.0117(2)
M5	0.99427(8)	0.34716(8)	0.29972(7)	24.4(1)	0.0161(8)
Si1	0.2045(1)	0.4506(1)	0.9105(1)		0.0066(2)
Si2	0.2121(1)	0.3656(1)	0.6542(1)		0.0059(2)
Si3	0.2154(1)	0.5786(1)	0.5308(1)		0.0068(2)
Si4	0.2122(1)	0.5072(1)	0.2632(1)		0.0068(2)
Si5	0.2039(1)	0.7007(1)	0.1248(1)		0.0065(2)
OA1	0.1271(3)	0.0697(3)	0.0406(3)		0.0088(5)
OA2	0.1187(3)	.1581(3)	0.3208(3)		0.0079(5)
OA3	0.1148(3)	0.9213(3)	0.4360(3)		0.0088(5)
OA4	0.1200(3)	0.0129(3)	0.7311(3)		0.0093(6)
OA5	0.1301(3)	0.7913(3)	0.8537(2)		0.0089(6)
OA6	0.0980(3)	0.8329(3)	0.1309(3)		0.0097(6)
OB1	0.1299(3)	0.3205(3)	0.9026(3)		0.0123(6)
OB2	0.1249(3)	0.2342(3)	0.6111(3)		0.0095(6)
OB3	0.1260(3)	0.7088(3)	0.5927(3)		0.0171(7)
OB4	0.1232(3)	0.3801(3)	0.1876(3)		0.0138(6)
OC1	0.1681(3)	0.4693(3)	0.7775(3)		0.0092(6)
OC2	0.1606(3)	0.4543(3)	0.5619(3)		0.0148(7)
OC3	0.1638(3)	0.5422(3)	0.3891(3)		0.0119(6)
OC4	0.1561(3)	0.6414(3)	0.2199(3)		0.0097(6)
OC5	0.1453(3)	0.5923(3)	0.9951(3)		0.0093(6)
15-4006					
M1	–0.00151(4	)0.03115(4)	0.14654(4)	24.92(7)	0.0074(1)
M2	0.00065(4)	0.12635(4)	0.44397(4)	24.59(7)	0.0077(1)
M3	0.01668(4)	0.20343(4)	0.72901(4)	24.54(7)	0.0075(1)
M4	0.06712(4)	0.26312(4)	0.02153(3)	27.45(7)	0.0111(1)
M5	0.99344(5)	0.35605(5)	0.30399(5)	21.85(7)	0.0127(2)
Si1	0.20479(7)	0.44854(7)	0.91124(6)		0.0058(1)
Si2	0.21323(7)	0.36551(7)	0.65358(6)		0.0053(1)
Si3	0.21695(7)	0.57884(7)	0.52862(6)		0.0058(1)
Si4	0.21289(7)	0.50576(7)	0.25926(7)		0.0062(1)
Si5	0.20225(7)	0.70063(7)	0.12368(6)		0.0060(1)
OA1	0.1271(2)	0.0731(2)	0.0394(2)		0.0081(3)
OA2	0.1184(2)	0.1581(2)	0.3219(2)		0.0077(3)
OA3	0.1138(2)	0.9230(2)	0.4368(2)		0.0083(3)
OA4	0.1201(2)	0.0134(2)	0.7327(2)		0.0081(3)
OA5	0.1330(2)	0.7907(2)	0.8537(2)		0.0086(3)
OA6	0.0956(2)	0.8321(2)	0.1278(2)		0.0099(4)
OB1	0.1298(2)	0.3183(2)	0.9017(2)		0.0101(4)
OB2	0.1253(2)	0.2346(2)	0.6102(2)		0.0090(3)
OB3	0.1302(2)	0.7111(2)	0.5880(2)		0.0130(4)
OB4	0.1240(2)	0.3799(2)	0.1799(2)		0.0111(4)

TABLE 5.—*Continued*

	x	*y*	*z*	e⁻	U_{eq}
OC1	0.1702(2)	0.4679(2)	0.7777(2)		0.0076(3)
OC2	0.1599(2)	0.4576(2)	0.5632(2)		0.0118(4)
OC3	0.1649(2)	0.5351(2)	0.3853(2)		0.0098(4)
OC4	0.1564(2)	0.6431(2)	0.2206(2)		0.0085(3)
OC5	0.1452(2)	0.5899(2)	0.9951(2)		0.0091(4)
15-4014					
M1	–0.00146(4)	0.03131(3)	0.14668(3)	24.81(7)	0.0079(1)
M2	0.00075(4)	0.12599(4)	0.44403(3)	24.65(6)	0.0080(1)
M3	0.01672(4)	0.20418(3)	0.72898(3)	24.64(6)	0.0081(1)
M4	0.06686(4)	0.26320(3)	0.02122(3)	27.36(6)	0.0114(1)
M5	0.99362(5)	0.35906(5)	0.30631(4)	20.66(6)	0.0104(1)
Si1	0.20495(6)	0.44901(6)	0.91116(6)		0.0065(1)
Si2	0.21321(6)	0.36630(6)	0.65340(6)		0.0058(1)
Si3	0.21794(6)	0.57993(6)	0.52844(6)		0.0061(1)
Si4	0.21385(6)	0.50566(6)	0.25871(6)		0.0066(1)
Si5	0.20233(7)	0.70059(6)	0.12362(6)		0.0068(1)
OA1	0.1274(2)	0.0730(2)	0.0397(2)		0.0091(3)
OA2	0.1188(2)	0.1577(2)	0.3225(2)		0.0088(3)
OA3	0.1134(2)	0.9230(2)	0.4366(2)		0.0085(3)
OA4	0.1196(2)	0.0136(2)	0.7328(2)		0.0089(3)
OA5	0.1331(2)	0.7902(2)	0.8530(2)		0.0093(3)
OA6	0.0954(2)	0.8314(2)	0.1276(2)		0.0097(3)
OB1	0.1298(2)	0.3196(2)	0.9014(2)		0.0105(3)
OB2	0.1260(2)	0.2359(2)	0.6100(2)		0.0098(3)
OB3	0.1316(2)	0.7125(2)	0.5867(2)		0.0110(3)
OB4	0.1256(2)	0.3803(2)	0.1794(2)		0.0108(3)
OC1	0.1706(2)	0.4680(2)	0.7776(2)		0.0087(3)
OC2	0.1595(2)	0.4597(2)	0.5639(2)		0.0098(3)
OC3	0.1663(2)	0.5346(2)	0.3850(2)		0.0101(3)
OC4	0.1566(2)	0.6426(2)	0.2202(2)		0.0091(3)
OC5	0.1455(2)	0.5899(2)	0.9951(2)		0.0099(3)
15-4020					
M1	–0.00166(6)	0.03116(5)	0.14652(5)	24.84(10)	0.0068(2)
M2	0.00066(6)	0.12629(5)	0.44394(5)	24.51(10)	0.0069(2)
M3	0.01659(6)	0.20350(5)	0.72902(5)	24.49(9)	0.0068(2)
M4	0.06736(6)	0.26305(5)	0.02148(4)	27.28(10)	0.0100(2)
M5	0.99327(7)	0.35632(7)	0.30409(7)	21.66(9)	0.0117(2)
Si1	0.20478(10)	0.44852(9)	0.91125(8)		0.0053(2)
Si2	0.21313(10)	0.36537(9)	0.65353(8)		0.0047(2)
Si3	0.21691(10)	0.57916(9)	0.52866(8)		0.0053(2)
Si4	0.21294(10)	0.50565(9)	0.25923(8)		0.0058(2)
Si5	0.20221(10)	0.70052(9)	0.1235(8)		0.0055(2)
OA1	0.1272(3)	0.0731(3)	0.0394(2)		0.0076(4)
OA2	0.1183(3)	0.1581(3)	0.3220(2)		0.0074(4)
OA3	0.1138(3)	0.9229(3)	0.4364(2)		0.0077(4)
OA4	0.1204(3)	0.0136(3)	0.7331(2)		0.0081(4)
OA5	0.1331(3)	0.7902(3)	0.8530(2)		0.0087(5)
OA6	0.0953(3)	0.8320(2)	0.1277(2)		0.0080(4)
OB1	0.1300(3)	0.3188(3)	0.9018(2)		0.0095(4)
OB2	0.1262(3)	0.2344(3)	0.6102(2)		0.0081(4)
OB3	0.1301(3)	0.7118(3)	0.5880(2)		0.0119(5)
OB4	0.1238(3)	0.3798(3)	0.1799(2)		0.0106(5)
OC1	0.1700(3)	0.4677(3)	0.7777(2)		0.0078(4)
OC2	0.1599(3)	0.4577(3)	0.5634(2)		0.0103(5)
OC3	0.1647(3)	0.5352(3)	0.3852(2)		0.0094(5)
OC4	0.1561(3)	0.6429(3)	0.2203(2)		0.0080(4)
OC5	0.1454(3)	0.5896(3)	0.9951(2)		0.0082(4)
15-4027					
M1	–0.00129(4)	0.03089(3)	0.14665(3)	24.54(6)	0.0073(1)
M2	0.00065(4)	0.12699(3)	0.44432(3)	24.24(6)	0.0076(1)
M3	0.01646(4)	0.20326(3)	0.72930(3)	24.20(6)	0.0072(1)
M4	0.06612(4)	0.26335(3)	0.02203(3)	26.46(6)	0.0111(1)
M5	0.99333(5)	0.35410(5)	0.30248(4)	22.60(6)	0.0139(1)
Si1	0.20482(6)	0.44858(6)	0.91140(5)		0.0059(1)
Si2	0.21307(6)	0.36507(6)	0.65394(5)		0.0053(1)
Si3	0.21659(6)	0.57849(6)	0.52910(5)		0.0059(1)
Si4	0.21250(6)	0.50579(6)	0.25977(5)		0.0061(1)
Si5	0.20261(6)	0.70071(6)	0.12396(5)		0.0060(1)
OA1	0.1273(2)	0.0733(2)	0.0393(1)		0.0083(3)
OA2	0.1185(2)	0.1585(2)	0.3216(1)		0.0082(3)
OA3	0.1143(2)	0.9226(2)	0.4365(1)		0.0084(3)
OA4	0.1206(2)	0.0134(2)	0.7329(2)		0.0089(3)
OA5	0.1325(2)	0.7899(2)	0.8537(1)		0.0083(3)
OA6	0.0959(2)	0.8322(2)	0.1281(2)		0.0088(3)
OB1	0.1298(2)	0.3187(2)	0.9021(1)		0.0098(3)
OB2	0.1255(2)	0.2343(2)	0.6110(1)		0.0093(3)
OB3	0.1291(2)	0.7100(2)	0.5894(2)		0.0148(3)

TABLE 5.—*Continued*

	x	y	z	e⁻	U_{eq}
OB4	0.1238(2)	0.3796(2)	0.1810(2)		0.0110(3)
OC1	0.1701(2)	0.4674(2)	0.7777(1)		0.0085(3)
OC2	0.1602(2)	0.4562(2)	0.5626(2)		0.0123(3)
OC3	0.1642(2)	0.5362(2)	0.3859(1)		0.0105(3)
OC4	0.1562(2)	0.6427(2)	0.2205(1)		0.0085(3)
OC5	0.1452(2)	0.5903(2)	0.9953(1)		0.0092(3)
15-4028					
M1	–0.00128(4)	0.03111(4)	0.14683(3)	24.84(7)	0.0066(1)
M2	0.00093(4)	0.12617(4)	0.44421(3)	24.74(7)	0.0066(1)
M3	0.01673(4)	0.20418(4)	0.72918(3)	24.70(7)	0.0066(1)
M4	0.06598(4)	0.26339(4)	0.02164(3)	26.85(7)	0.0102(1)
M5	0.99395(5)	0.35807(5)	0.30592(4)	20.98(6)	0.0102(1)
Si1	0.20500(7)	0.44935(6)	0.91108(6)		0.0051(1)
Si2	0.21304(7)	0.36632(6)	0.65348(6)		0.0047(1)
Si3	0.21770(7)	0.57982(6)	0.52867(6)		0.0047(1)
Si4	0.21395(7)	0.50607(7)	0.2594(6)		0.0054(1)
Si5	0.20285(7)	0.70063(6)	0.12388(6)		0.0054(1)
OA1	0.1270(2)	0.0722(2)	0.0397(2)		0.0075(3)
OA2	0.1188(2)	0.1577(2)	0.3225(2)		0.0074(3)
OA3	0.1135(2)	0.9230(2)	0.4365(2)		0.0076(3)
OA4	0.1194(2)	0.0131(2)	0.7325(2)		0.0078(3)
OA5	0.1329(2)	0.7901(2)	0.8529(2)		0.0078(3)
OA6	0.0957(2)	0.8320(2)	0.1284(2)		0.0088(3)
OB1	0.1298(2)	0.3200(2)	0.9015(2)		0.0092(3)
OB2	0.1254(2)	0.2360(2)	0.6102(2)		0.0080(3)
OB3	0.1310(2)	0.7122(2)	0.5872(2)		0.0104(3)
OB4	0.1258(2)	0.3807(2)	0.1804(2)		0.0102(3)
OC1	0.1706(2)	0.4686(2)	0.7777(2)		0.0075(3)
OC2	0.1597(2)	0.4592(2)	0.5635(2)		0.0093(3)
OC3	0.1662(2)	0.5354(2)	0.3855(2)		0.0092(3)
OC4	0.1571(2)	0.6423(2)	0.2203(2)		0.0078(3)
OC5	0.1457(2)	0.5907(2)	0.99514(2)		0.0081(3)
15-4029					
M1	–0.00119(4)	0.03115(3)	0.14686(3)	24.91(6)	0.0073(1)
M2	0.00090(4)	0.12570(3)	0.44400(3)	24.67(6)	0.0071(1)
M3	0.01673(4)	0.20471(3)	0.72902(3)	24.64(6)	0.0076(1)
M4	0.06622(4)	0.26336(3)	0.02146(3)	26.98(6)	0.0111(1)
M5	0.99400(5)	0.35950(5)	0.30700(4)	20.41(6)	0.0094(1)
Si1	0.20494(6)	0.44933(6)	0.91094(5)		0.0057(1)
Si2	0.21318(6)	0.36657(6)	0.65330(5)		0.0053(1)
Si3	0.21805(6)	0.58031(6)	0.52835(5)		0.0054(1)
Si4	0.21443(6)	0.50584(6)	0.25906(5)		0.0059(1)
Si5	0.20289(6)	0.70043(6)	0.12364(5)		0.0062(1)
OA1	0.1277(2)	0.0722(2)	0.0399(2)		0.0083(3)
OA2	0.1192(2)	0.1575(2)	0.3228(1)		0.0076(3)
OA3	0.1132(2)	0.9231(2)	0.4366(2)		0.0084(3)
OA4	0.1191(2)	0.0137(2)	0.7329(2)		0.0082(3)
OA5	0.1328(2)	0.7905(2)	0.8529(1)		0.0083(3)
OA6	0.0957(2)	0.8318(2)	0.1282(2)		0.0092(3)
OB1	0.1298(2)	0.3200(2)	0.9013(2)		0.0100(3)
OB2	0.1257(2)	0.2364(2)	0.6097(1)		0.0087(3)
OB3	0.1319(2)	0.7130(2)	0.5867(2)		0.0100(3)
OB4	0.1265(2)	0.3806(2)	0.1801(2)		0.0103(3)
OC1	0.1705(2)	0.4681(2)	0.7775(1)		0.0083(3)
OC2	0.1592(2)	0.4605(2)	0.5639(1)		0.0086(3)
OC3	0.1668(2)	0.5349(2)	0.3850(1)		0.0088(3)
OC4	0.1573(2)	0.6425(2)	0.2199(1)		0.0079(3)
OC5	0.1460(2)	0.5905(2)	0.9947(1)		0.0091(3)
15-4040					
M1	–0.00133(6)	0.03117(6)	0.14679(5)	24.8(1)	0.0060(2)
M2	0.00086(6)	0.12602(6)	0.44416(5)	24.9(1)	0.0064(2)
M3	0.01677(6)	0.20416(6)	0.72909(5)	24.8(1)	0.0062(2)
M4	0.06627(6)	0.26327(6)	0.02146(5)	27.0(1)	0.0096(2)
M5	0.99385(8)	0.35827(8)	0.30602(7)	20.9(1)	0.0096(2)
Si1	0.2052(1)	0.4494(1)	0.9112(1)		0.0047(2)
Si2	0.2131(1)	0.3665(1)	0.6536(1)		0.0042(2)
Si3	0.2179(1)	0.5797(1)	0.5286(1)		0.0044(2)
Si4	0.2139(1)	0.5059(1)	0.2591(1)		0.0048(2)
Si5	0.2028(1)	0.7006(1)	0.1238(1)		0.0051(2)
OA1	0.1275(3)	0.0726(3)	0.0401(2)		0.0079(5)
OA2	0.1189(3)	0.1582(3)	0.3227(2)		0.0066(5)
OA3	0.1139(3)	0.9232(3)	0.4367(2)		0.0073(5)
OA4	0.1198(3)	0.0137(3)	0.7330(2)		0.0070(5)
OA5	0.1332(3)	0.7899(3)	0.8525(2)		0.0079(5)
OA6	0.0954(3)	0.8321(3)	0.1283(3)		0.0085(5)
OB1	0.1301(3)	0.3191(3)	0.9010(2)		0.0090(5)

TABLE 5.—*Continued*

	x	y	z	e⁻	U_{eq}
OB2	0.1258(3)	0.2360(3)	0.6103(2)		0.0083(5)
OB3	0.1313(3)	0.7122(3)	0.5869(3)		0.0103(5)
OB4	0.1261(3)	0.3806(3)	0.1805(3)		0.0103(5)
OC1	0.1702(3)	0.4681(3)	0.7774(2)		0.0072(5)
OC2	0.1591(3)	0.4595(3)	0.5638(2)		0.0079(5)
OC3	0.1664(3)	0.5352(3)	0.3851(2)		0.0085(5)
OC4	0.1571(3)	0.6428(3)	0.2201(2)		0.0071(5)
OC5	0.1449(3)	0.5902(3)	0.9948(2)		0.0079(5)
15-4041					
M1	–0.00130(4)	0.03113(4)	0.14693(3)	24.51(7)	0.0056(1)
M2	0.00087(4)	0.12580(4)	0.44409(3)	24.34(7)	0.0056(1)
M3	0.01664(4)	0.20497(4)	0.72913(3)	24.33(7)	0.0057(1)
M4	0.06617(4)	0.26347(4)	0.02144(3)	26.79(7)	0.0091(1)
M5	0.99374(5)	0.35973(5)	0.30711(5)	20.20(6)	0.0074(1)
Si1	0.20513(7)	0.44941(7)	0.91111(6)		0.0046(1)
Si2	0.21346(7)	0.36663(7)	0.65328(6)		0.0037(1)
Si3	0.21825(7)	0.58031(7)	0.52835(6)		0.0038(1)
Si4	0.21433(7)	0.50576(7)	0.25898(6)		0.0043(1)
Si5	0.20267(7)	0.70038(7)	0.12354(6)		0.0044(1)
OA1	0.1275(2)	0.0724(2)	0.0400(2)		0.0065(3)
OA2	0.1192(2)	0.1576(2)	0.3230(2)		0.0065(3)
OA3	0.1135(2)	0.9229(2)	0.4367(2)		0.0064(3)
OA4	0.1192(2)	0.0137(2)	0.7328(2)		0.0070(3)
OA5	0.1333(2)	0.7905(2)	0.8531(2)		0.0071(3)
OA6	0.0955(2)	0.8310(2)	0.1281(2)		0.0076(3)
OB1	0.1303(2)	0.3206(2)	0.9018(2)		0.0086(3)
OB2	0.1261(2)	0.2364(2)	0.6095(2)		0.0083(3)
OB3	0.1320(2)	0.7128(2)	0.5868(2)		0.0082(3)
OB4	0.1264(2)	0.3802(2)	0.1799(2)		0.0087(3)
OC1	0.1705(2)	0.4683(2)	0.7774(2)		0.0072(3)
OC2	0.1593(2)	0.4607(2)	0.5640(2)		0.0070(3)
OC3	0.1665(2)	0.5352(2)	0.3851(2)		0.0071(3)
OC4	0.1574(2)	0.6417(2)	0.2196(2)		0.0067(3)
OC5	0.1459(2)	0.5906(2)	0.9948(2)		0.0079(3)

second principle component, which accounts for nearly the other half the variance in the data, represents an expected antipathetic relationship between Mn and Fe, which probably occurs at all M sites.

For the principal component analysis of fowlerite compositions (Table 10b), we included all five M-site cations. The first principle component, accounting for over half of the variance in the fowlerite compositional data, appears to represent an antipathetic relation between (Zn,Mg) and Ca. Given the implications of the X-ray site refinements (Table 9) and the contrasting ionic radii, it seems unlikely that this represents direct cationic substitution of Zn + Mg for Ca at any particular M site. We interpret it as a reflection of the compositional trends in fowlerite seen in Figure 2, probably driven by the bulk compositions of the rocks at Franklin, New Jersey. The second principle component shows the same antipathetic relationship between Mn and Fe as seen in typical rhodonite. The first two principal components account for 90% of the total variance in the data.

Whereas the assignment of cations to M sites and identification of cationic substitutions are somewhat ambiguous for both rhodonite and fowlerite, it is clear that the patterns of substitutions revealed by the first principal components of both compositional data sets, and implied by X-ray site refinements, are different. Thus, the crystal chemistry of fowlerite may not be correctly characterized and understood by considering it to be merely a Zn-rich rhodonite.

Crystallographic relationships

Figure 3 shows correlations among unit-cell edges and interaxial angles for the sixteen specimens for which we obtained crys-

TABLE 7. Selected interatomic distances (Å)

Specimen:	15-4018	15-4024	15-4025	15-4026	15-4030	15-4031	15-4033	15-4034
M1-OA5	2.133(2)	2.136(3)	2.140(4)	2.130(6)	2.135(3)	2.139(3)	2.118(3)	2.121(3)
M1-OA6	2.140(2)	2.130(3)	2.129(4)	2.136(6)	2.145(3)	2.135(3)	2.123(3)	2.124(3)
M1-OA1	2.184(2)	2.167(3)	2.174(4)	2.173(6)	2.182(3)	2.172(3)	2.168(3)	2.166(3)
M1-OA4	2.261(2)	2.263(3)	2.258(4)	2.260(6)	2.259(3)	2.254(3)	2.259(3)	2.258(3)
M1-OA2	2.273(3)	2.267(3)	2.268(4)	2.268(6)	2.279(3)	2.266(3)	2.263(3)	2.267(3)
M1-OA1	2.341(2)	2.335(3)	2.341(4)	2.328(6)	2.347(3)	2.341(3)	2.324(3)	2.325(3)
M2-OB3	2.086(3)	2.109(4)	2.101(4)	2.098(6)	2.090(4)	2.088(3)	2.093(3)	2.093(3)
M2-OB2	2.166(2)	2.155(3)	2.158(4)	2.150(6)	2.159(3)	2.161(3)	2.155(3)	2.153(3)
M2-OA2	2.217(2)	2.220(3)	2.222(4)	2.221(5)	2.224(3)	2.215(3)	2.215(3)	2.218(3)
M2-OA3	2.251(3)	2.249(3)	2.251(4)	2.249(6)	2.254(3)	2.246(3)	2.256(3)	2.246(3)
M2-OA3	2.266(2)	2.298(3)	2.285(4)	2.281(6)	2.267(3)	2.279(3)	2.261(3)	2.275(3)
M2-OA4	2.341(3)	2.358(3)	2.350(4)	2.347(6)	2.345(3)	2.344(3)	2.330(3)	2.338(3)
M3-OB2	2.117(3)	2.099(3)	2.104(4)	2.103(6)	2.121(3)	2.113(3)	2.107(3)	2.102(3)
M3-OA4	2.131(2)	2.126(3)	2.130(4)	2.121(5)	2.133(3)	2.131(3)	2.119(3)	2.117(3)
M3-OB1	2.195(3)	2.207(3)	2.212(4)	2.194(6)	2.200(3)	2.196(3)	2.196(3)	2.198(3)
M3-OC4	2.245(2)	2.249(3)	2.251(4)	2.240(6)	2.254(3)	2.246(3)	2.233(3)	2.231(3)
M3-OA3	2.254(3)	2.243(3)	2.252(4)	2.250(6)	2.257(3)	2.254(3)	2.246(3)	2.244(3)
M3-OA6	2.404(3)	2.386(3)	2.389(4)	2.385(6)	2.404(3)	2.396(3)	2.392(3)	2.386(3)
M4-OB4	1.965(3)	1.988(3)	1.987(4)	1.976(6)	1.973(3)	1.969(3)	1.970(3)	1.972(3)
M4-OB1	2.052(3)	2.052(3)	2.054(4)	2.049(6)	2.053(3)	2.042(3)	2.051(3)	2.042(3)
M4-OA1	2.117(2)	2.117(3)	2.114(4)	2.118(6)	2.120(3)	2.113(3)	2.107(3)	2.105(3)
M4-OA6	2.212(3)	2.228(3)	2.226(4)	2.228(6)	2.213(3)	2.218(3)	2.220(3)	2.222(3)
M4-OC5	2.374(2)	2.362(3)	2.362(4)	2.360(6)	2.364(3)	2.364(3)	2.368(3)	2.372(3)
M4-OA5	2.874(3)	2.818(3)	2.849(4)	2.843(6)	2.864(3)	2.842(3)	2.864(3)	2.854(3)
M5-OA5	2.270(3)	2.175(3)	2.198(4)	2.205(6)	2.280(3)	2.242(3)	2.214(3)	2.189(3)
M5-OB4	2.273(3)	2.167(3)	2.198(4)	2.196(6)	2.290(4)	2.248(3)	2.218(3)	2.188(3)
M5-OB3	2.286(3)	2.163(4)	2.209(5)	2.206(7)	2.293(4)	2.249(3)	2.228(4)	2.199(4)
M5-OA2	2.308(2)	2.230(3)	2.254(4)	2.251(6)	2.318(3)	2.290(3)	2.255(3)	2.240(3)
M5-OC3	2.532(3)	2.631(4)	2.606(4)	2.606(6)	2.526(3)	2.544(3)	2.577(3)	2.603(3)
M5-OC1	2.587(2)	2.631(3)	2.607(4)	2.624(6)	2.588(3)	2.598(3)	2.596(3)	2.603(3)
M5-OC2	2.657(3)	2.780(4)	2.742(4)	2.738(7)	2.645(4)	2.682(3)	2.724(4)	2.748(4)
Si1-OB1	1.592(3)	1.593(3)	1.591(4)	1.600(6)	1.594(3)	1.594(3)	1.593(3)	1.598(3)
Si1-OA1	1.627(3)	1.627(3)	1.627(4)	1.626(6)	1.626(3)	1.630(3)	1.635(3)	1.627(3)
Si1-OC5	1.640(3)	1.638(3)	1.643(4)	1.641(6)	1.642(3)	1.638(3)	1.641(3)	1.635(3)
Si1-OC1	1.660(3)	1.655(3)	1.657(4)	1.648(6)	1.660(3)	1.658(3)	1.654(3)	1.652(3)
Si2-OB2	1.596(3)	1.596(3)	1.599(4)	1.608(6)	1.604(3)	1.594(3)	1.600(3)	1.596(3)
Si2-OA2	1.615(3)	1.613(3)	1.614(4)	1.610(6)	1.610(3)	1.614(3)	1.619(3)	1.610(3)
Si2-OC2	1.650(3)	1.642(3)	1.638(4)	1.630(6)	1.650(3)	1.643(3)	1.638(3)	1.636(3)
Si2-OC1	1.662(3)	1.660(3)	1.664(4)	1.657(6)	1.661(3)	1.663(3)	1.661(3)	1.662(3)
Si3-OB3	1.585(3)	1.593(4)	1.591(4)	1.586(6)	1.583(4)	1.587(3)	1.585(3)	1.588(3)
Si3-OA3	1.615(3)	1.613(3)	1.612(4)	1.618(6)	1.612(3)	1.611(3)	1.615(3)	1.615(3)
Si3-OC3	1.633(3)	1.627(3)	1.624(4)	1.619(6)	1.632(3)	1.630(3)	1.627(3)	1.622(3)
Si3-OC2	1.666(3)	1.641(3)	1.658(4)	1.664(6)	1.667(3)	1.657(3)	1.660(3)	1.651(3)
Si4-OB4	1.592(3)	1.592(4)	1.593(4)	1.602(6)	1.585(4)	1.587(3)	1.594(3)	1.595(3)
Si4-OA4	1.613(3)	1.604(3)	1.613(4)	1.612(6)	1.614(3)	1.610(3)	1.615(3)	1.611(3)
Si4-OC3	1.633(3)	1.625(3)	1.631(4)	1.627(6)	1.635(3)	1.633(3)	1.629(3)	1.628(3)
Si4-OC4	1.648(3)	1.639(3)	1.636(4)	1.646(6)	1.641(3)	1.641(3)	1.641(3)	1.643(3)
Si5-OA5	1.591(3)	1.595(3)	1.595(4)	1.593(6)	1.589(3)	1.590(3)	1.596(3)	1.592(3)
Si5-OA6	1.616(3)	1.610(3)	1.618(4)	1.607(6)	1.610(3)	1.614(3)	1.612(3)	1.607(3)
Si5-OC5	1.654(3)	1.654(3)	1.655(4)	1.652(6)	1.656(3)	1.655(3)	1.652(3)	1.655(3)
Si5-OC4	1.655(3)	1.655(3)	1.657(4)	1.654(6)	1.660(3)	1.654(3)	1.661(3)	1.657(3)

tal structure refinements (Table 4). The following observations may be made: (1) despite the limited geographical occurrence of fowlerite, it exhibits a range in lattice parameters comparable to that of typical rhodonite; (2) correlations among cell edges are better developed for fowlerite than for rhodonite; (3) among the cell edges, *a* discriminates most effectively between Zn-rich and Zn-poor specimens; and (4) the interaxial angles are more effective than the cell edges in discriminating between rhodonite and fowlerite, with no overlap in the range of β between fowlerite and rhodonite for our sixteen structure-refined specimens. The maximum rhodonite and minimum fowlerite β values for our specimens are 103.335(2)° and 103.597(3)°, respectively. This is consistent with the 103.6° minimum value of β observed in Zn-rich rhodonite by Viswanathan and Harneit (1986).

The grand mean M-O and Si-O distances are essentially identical: 2.242 and 1.625 Å, respectively, for the rhodonite specimens, and 2.241 and 1.627 Å, respectively, for the fowlerite specimens. Differences between the Zn-poor and Zn-rich groups become apparent upon examination of the mean bond lengths for individual M sites, which are given in Table 11. Table 12 displays the simple correlation coefficients between unit-cell parameters and M-O bond lengths (with M4 and M5 in six- and seven-coordination, respectively), and reveals clearly different characteristics for fowlerite and rhodonite. For rhodonite, <M1-O>, <M3-O>, and <M5-O> are strongly correlated with *a* and *b*, but not with *c*. Correlations between <M2-O> and cell edges are insignificant, but are rather strong with all three interaxial angles. <M4-O> for rhodonite shows no strong correlations with cell parameters. For fowlerite, four out of five of the mean M-O bond lengths (including <M4-O>) are strongly correlated with all three unit cell edges. Only <M2-O> shows no significant correlation with cell edges, and unlike in rhodonite, it is not correlated strongly with interaxial angles, either.

Figure 4 shows the electron population at each M site as a

TABLE 7.—*Continued*

Specimen:	15-4006	15-4014	15-4020	15-4027	15-4028	15-4029	15-4040	15-4041
M1-OA5	2.123(2)	2.131(2)	2.125(3)	2.133(3)	2.134(2)	2.1306(2)	2.135(3)	2.136(2)
M1-OA6	2.141(2)	2.151(2)	2.140(2)	2.133(3)	2.146(2)	2.1476(2)	2.144(3)	2.157(2)
M1-OA1	2.195(2)	2.199(2)	2.195(3)	2.192(3)	2.191(2)	2.1969(2)	2.194(3)	2.199(2)
M1-OA4	2.271(2)	2.275(2)	2.269(3)	2.272(3)	2.270(2)	2.2698(2)	2.272(3)	2.273(2)
M1-OA2	2.270(2)	2.276(2)	2.270(3)	2.267(3)	2.275(2)	2.280(2)	2.280(3)	2.282(2)
M1-OA1	2.307(2)	2.315(2)	2.305(3)	2.310(3)	2.314(2)	2.320(2)	2.320(3)	2.322(2)
M2-OB3	2.075(2)	2.073(2)	2.069(3)	2.086(3)	2.076(2)	2.075(2)	2.077(3)	2.079(2)
M2-OB2	2.158(2)	2.162(2)	2.154(3)	2.153(3)	2.159(2)	2.163(2)	2.163(3)	2.162(2)
M2-OA2	2.219(2)	2.220(2)	2.215(3)	2.224(3)	2.217(2)	2.219(2)	2.220(3)	2.219(2)
M2-OA3	2.253(2)	2.252(2)	2.252(3)	2.255(3)	2.254(2)	2.248(2)	2.253(3)	2.256(2)
M2-OA3	2.256(2)	2.257(2)	2.256(3)	2.266(3)	2.256(2)	2.256(2)	2.259(3)	2.257(2)
M2-OA4	2.337(2)	2.337(2)	2.336(3)	2.343(3)	2.335(2)	2.337(2)	2.342(3)	2.339(2)
M3-OB2	2.117(2)	2.133(2)	2.124(3)	2.116(3)	2.127(2)	2.135(2)	2.129(3)	2.142(2)
M3-OA4	2.120(2)	2.128(2)	2.120(2)	2.120(3)	2.131(2)	2.132(2)	2.128(3)	2.137(2)
M3-OB1	2.185(2)	2.184(2)	2.183(3)	2.185(3)	2.185(2)	2.185(2)	2.181(3)	2.192(2)
M3-OC4	2.233(2)	2.239(2)	2.230(2)	2.235(3)	2.243(2)	2.244(2)	2.241(3)	2.250(2)
M3-OA3	2.239(2)	2.244(2)	2.235(3)	2.240(3)	2.246(2)	2.248(2)	2.249(3)	2.251(2)
M3-OA6	2.418(2)	2.429(2)	2.420(3)	2.411(3)	2.420(2)	2.429(2)	2.423(3)	2.426(2)
M4-OB4	1.928(2)	1.930(2)	1.923(3)	1.933(3)	1.938(2)	1.938(2)	1.941(3)	1.935(2)
M4-OB1	1.980(2)	1.994(2)	1.982(3)	1.986(3)	2.003(2)	2.003(2)	2.002(3)	2.005(2)
M4-OA1	2.067(2)	2.075(2)	2.065(3)	2.069(3)	2.085(2)	2.088(2)	2.082(3)	2.090(2)
M4-OA6	2.180(2)	2.180(2)	2.181(3)	2.184(3)	2.188(2)	2.188(2)	2.186(3)	2.184(2)
M4-OC5	2.429(2)	2.435(2)	2.434(3)	2.424(3)	2.424(2)	2.430(2)	2.424(3)	2.431(2)
M4-OA5	2.968(2)	2.980(2)	2.972(3)	2.945(2)	2.966(2)	2.975(2)	2.977(3)	2.981(2)
M5-OA5	2.256(2)	2.289(2)	2.254(3)	2.235(3)	2.282(2)	2.299(2)	2.282(3)	2.305(2)
M5-OB4	2.292(2)	2.328(2)	2.293(3)	2.269(3)	2.316(2)	2.332(2)	2.320(3)	2.335(2)
M5-OB3	2.307(2)	2.338(2)	2.306(3)	2.274(4)	2.325(2)	2.342(2)	2.331(3)	2.342(2)
M5-OA2	2.309(2)	2.342(2)	2.313(3)	2.289(3)	2.333(2)	2.348(2)	2.332(3)	2.353(2)
M5-OC3	2.502(2)	2.489(2)	2.496(3)	2.526(3)	2.498(2)	2.491(2)	2.499(3)	2.493(2)
M5-OC1	2.570(2)	2.565(2)	2.568(3)	2.585(3)	2.570(2)	2.568(2)	2.568(3)	2.566(2)
M5-OC2	2.653(2)	2.615(2)	2.648(3)	2.690(3)	2.629(2)	2.606(2)	2.620(3)	2.605(2)
Si1-OB1	1.598(2)	1.598(2)	1.594(3)	1.596(4)	1.597(2)	1.599(2)	1.604(3)	1.595(2)
Si1-OA1	1.630(2)	1.633(2)	1.631(3)	1.629(3)	1.634(2)	1.630(2)	1.629(3)	1.632(2)
Si1-OC5	1.631(2)	1.632(2)	1.628(3)	1.632(3)	1.635(2)	1.632(2)	1.633(3)	1.635(2)
Si1-OC1	1.655(2)	1.657(2)	1.655(3)	1.659(3)	1.656(2)	1.655(2)	1.659(3)	1.660(2)
Si2-OB2	1.596(2)	1.596(2)	1.594(3)	1.596(4)	1.598(2)	1.597(2)	1.598(3)	1.599(2)
Si2-OA2	1.611(2)	1.613(2)	1.612(3)	1.613(4)	1.613(2)	1.610(2)	1.613(3)	1.610(2)
Si2-OC2	1.643(2)	1.647(2)	1.641(3)	1.637(3)	1.648(2)	1.651(2)	1.648(3)	1.653(2)
Si2-OC1	1.663(2)	1.662(2)	1.662(3)	1.659(3)	1.663(2)	1.662(2)	1.659(3)	1.664(2)
Si3-OB3	1.582(2)	1.582(2)	1.584(3)	1.583(3)	1.583(2)	1.582(2)	1.582(3)	1.584(2)
Si3-OA3	1.617(2)	1.616(2)	1.617(3)	1.614(4)	1.617(2)	1.618(2)	1.612(3)	1.615(2)
Si3-OC3	1.627(2)	1.632(2)	1.631(3)	1.628(3)	1.629(2)	1.632(2)	1.634(3)	1.632(2)
Si3-OC2	1.665(2)	1.673(2)	1.666(3)	1.665(3)	1.668(2)	1.672(2)	1.672(3)	1.673(2)
Si4-OB4	1.592(2)	1.591(2)	1.595(3)	1.590(3)	1.591(2)	1.589(2)	1.587(3)	1.594(2)
Si4-OA4	1.611(2)	1.611(2)	1.608(3)	1.610(4)	1.612(2)	1.612(2)	1.610(3)	1.613(2)
Si4-OC3	1.640(2)	1.643(2)	1.637(3)	1.634(3)	1.640(2)	1.640(2)	1.638(3)	1.642(2)
Si4-OC4	1.643(2)	1.644(2)	1.645(3)	1.642(3)	1.640(2)	1.645(2)	1.646(3)	1.642(2)
Si5-OA5	1.591(2)	1.594(2)	1.588(3)	1.586(4)	1.588(2)	1.591(2)	1.587(3)	1.589(2)
Si5-OA6	1.610(2)	1.610(2)	1.610(3)	1.619(3)	1.615(2)	1.616(2)	1.618(3)	1.613(2)
Si5-OC5	1.649(2)	1.650(2)	1.647(3)	1.650(3)	1.650(2)	1.652(2)	1.656(3)	1.650(2)
Si5-OC4	1.659(2)	1.662(2)	1.659(3)	1.660(3)	1.661(2)	1.659(2)	1.657(3)	1.660(2)

function of the β angle, which we have previously shown (Fig. 3) discriminates between rhodonite and fowlerite. The electron populations at M1, M2, and M3 vary little across our specimens, and the principal differences are at M4 and M5. The plot would look very similar if electronegativity were substituted for electron population. Thus the major crystal-chemical differences between rhodonite and fowlerite are likely associated with M4 and M5, and we examine them in detail below.

The M4 and M5 sites

Zn preferentially occupies M4, so we expect major crystallochemical differences between rhodonite and fowlerite to be associated with that site. By virtually any measure, M4 is the most distorted of the M sites in rhodonite. In rhodonite, it has been described as an octahedron (Dickson 1975) and as a five-coordinated site (Ohashi and Finger 1975; Peacor and Niizeki 1963; Peacor et al. 1978; Pinckney and Burnham 1988), with reasonable justification for each characterization. Figure 5 shows the number of electrons at M4, derived from our 16 X-ray site refinements, as a function of octahedral angle variance (Robinson et al. 1971), a measure of octahedral distortion. The plot includes points for the Mg-rich rhodonites of Peacor et al. (1978) and Murakami and Takéuchi (1979), with the number of electrons being calculated on the basis of site refinements reported by the respective authors. The curve is quadratic, and the fit is obviously very good. Because the mean cation size at M4 is larger for our rhodonite specimens than for either the fowlerite specimens or the Mg-rich rhodonites, this correlation cannot be ascribed to the influence of cation size on the geometry of M4. This relationship will be further discussed after examination of the distortion at the M4 site.

Figure 6a depicts the M4 site, showing the nearest six neighbors to the cation (at the scale of this diagram, the M4 sites of rhodonite and fowlerite appear identical to the eye). The square is at the location of the centroid defined by the locations of the six oxygen atoms. It is clear that the cation is markedly closer

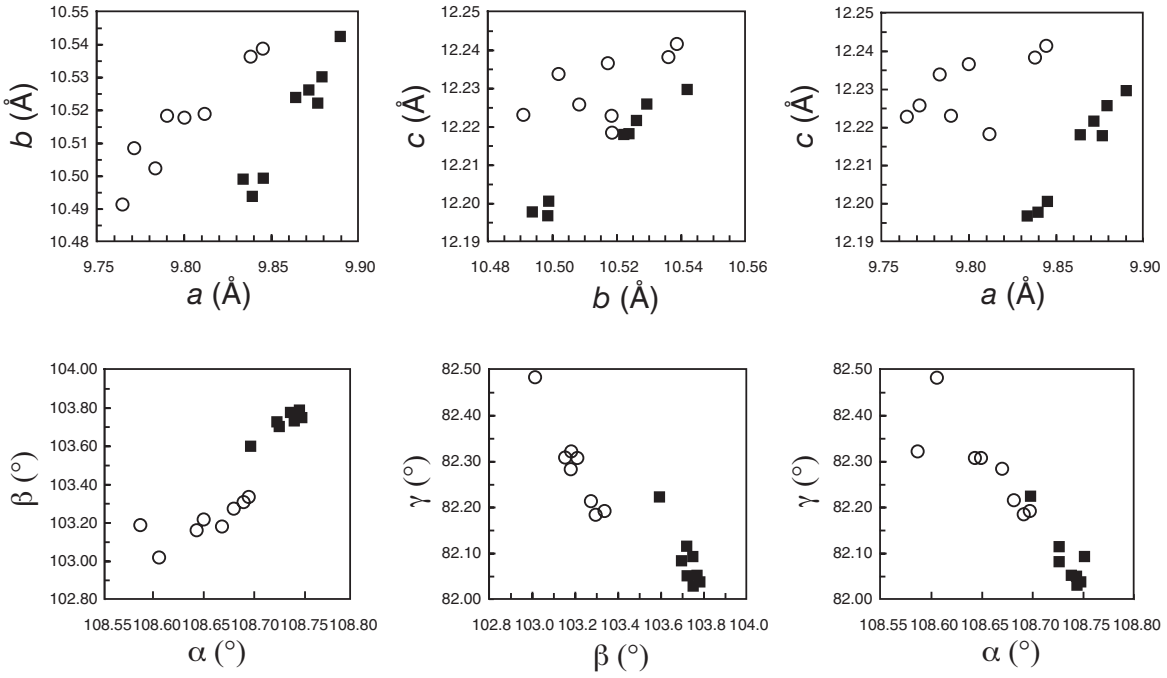

FIGURE 3. Relationships among unit-cell parameters (rhodonite = open circles, fowlerite = filled squares).

to one "apical" oxygen atom than to the other, and that there is a reasonable geometrical basis for considering M4 to be five coordinated. For our eight rhodonite specimens, the average distance from the centroid to the cation is 0.506(3) Å, and for our eight fowlerite specimens, that distance is 0.563(2) Å. Thus the tendency toward five coordination for M4 is markedly stronger in fowlerite than it is in rhodonite.

Figure 6b shows the seven nearest-neighbor oxygen atoms of the M4 site in fowlerite, with the three most distant shown with subdued shading. The four nearest oxygen atoms form a crude but quite obvious tetrahedron about the M4 cation. Whereas octahedrally coordinated Zn is by no means uncommon, the preference of Zn for tetrahedral coordination in oxides, sulfides, chlorides, and bromides has been noted by several workers (e.g., Evans 1966; Mihaljevic 1999). Zn occurs in tetrahedral coordination in zincite (Abrahams and Bernstein 1969; Smyth et al. 2000), staurolite (Griffen and Ribbe 1973; Griffen 1981), hemimorphite (Libowitzky et al. 1998), parahopeite (Chao 1969), hardystonite (Louisnathan 1969; Bindi et al. 2001), veszelyite (Ghose et al. 1974), gahnite (O'Neill and Dollase 1994), franklinite (Lucchesi et al. 1999), $CaZnSi_3O_8$ "feldspar" (Fehr 2001), and many other Zn-containing minerals and inorganic compounds. The trend toward tetrahedral coordination in fowlerite appears clearly in Figure 7. The behavior of the three longest bond lengths for each group in Figure 7 suggests that, as in Figure 5, the relationships shown here are not solely a function of cation size.

The replacement of electron population in Figure 5 by mean electronegativity of the cation at M4 yields Figure 8. Mean electronegativities were obtained by (1) constructing "plausible" cation site assignments for each specimen by the methods used for Table 9, and (2) calculating the weighted average electronegativity based on the values of Allred (1961). In doing this, Fe

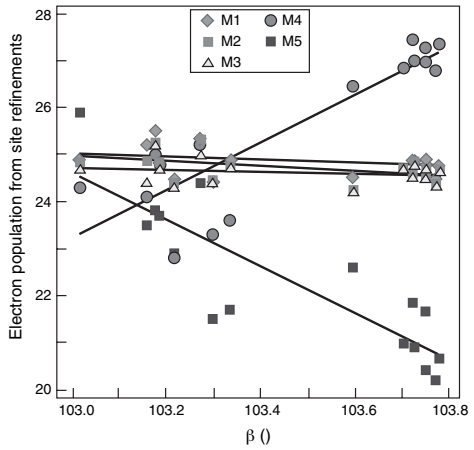

FIGURE 4. β angle as a function of electron population at the M sites. The trend lines are least-squares fits.

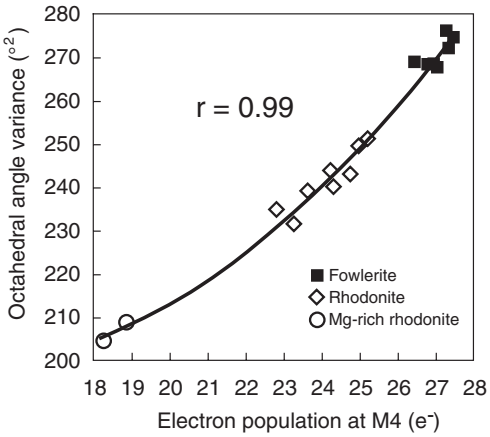

FIGURE 5. Octahedral angle variance (σ_o^2) at M4 as a function of electron population from site refinements.

TABLE 8. Selected bond angles (°)

Specimen:	15-4018	15-4024	15-4025	15-4026
OA6-M1-OA1	92.3(1)	92.1(1)	92.3(2)	92.2(2)
OA5-M1-OA1	91.6(1)	90.7(1)	91.2(1)	91.2(2)
OA6-M1-OA4	85.8(1)	86.6(1)	86.3(2)	86.0(2)
OA5-M1-OA4	90.9(1)	91.2(1)	90.9(2)	91.1(2)
OA6-M1-OA2	103.9(1)	104.1(1)	104.2(2)	103.9(2)
OA5-M1-OA2	85.1(1)	84.6(1)	84.5(1)	84.7(2)
OA1-M1-OA2	95.3(1)	94.9(1)	95.0(1)	95.1(2)
OA4-M1-OA2	81.7(1)	82.1(1)	82.0(1)	82.1(2)
OA6-M1-OA1	83.8(1)	84.5(1)	84.2(1)	84.5(2)
OA5-M1-OA1	87.6(1)	87.2(1)	87.6(1)	87.3(2)
OA1-M1-OA1	80.0(1)	79.1(1)	79.3(2)	79.2(2)
OA4-M1-OA1	103.3(1)	104.1(1)	104.1(1)	103.9(2)
OB3-M2-OB2	97.6(1)	99.1(1)	98.9(2)	98.4(2)
OB3-M2-OA2	84.6(1)	81.7(1)	82.8(2)	82.8(2)
OB2-M2-OA2	99.8(1)	101.0(1)	100.7(2)	100.6(2)
OB3-M2-OA3	99.1(1)	101.8(1)	100.8(2)	100.9(2)
OB2-M2-OA3	82.4(1)	81.6(1)	81.9(1)	81.8(2)
OB2-M2-OA3	97.1(1)	96.2(1)	96.4(2)	96.5(2)
OA2-M2-OA3	91.9(1)	91.5(1)	91.7(1)	91.9(2)
OA3-M2-OA3	83.9(1)	84.4(1)	84.0(2)	83.8(2)
OB3-M2-OA4	88.5(1)	88.1(1)	88.0(2)	88.6(2)
OA2-M2-OA4	81.2(1)	81.0(1)	80.9(1)	81.2(2)
OA3-M2-OA4	96.3(1)	96.0(1)	96.0(1)	96.0(2)
OA3-M2-OA4	76.9(1)	76.6(1)	76.8(1)	76.6(2)
OB2-M3-OA4	96.5(1)	95.2(1)	95.8(2)	95.8(2)
OB2-M3-OB1	102.8(1)	103.3(1)	103.0(2)1	03.5(2)
OA4-M3-OB1	97.8(1)	97.0(1)	97.5(2)	97.6(2)
OB2-M3-OA3	83.4(1)	83.0(1)	83.1(2)	82.8(2)
OA4-M3-OA3	81.5(1)	82.7(1)	81.4(1)	82.0(2)
OB2-M3-OC4	115.7(1)	115.2(1)	115.3(2)	115.3(2)
OB1-M3-OC4	81.9(1)	81.7(1)	82.1(2)	81.5(2)
OA3-M3-OC4	95.4(1)	95.4(1)	95.7(1)	95.5(2)
OA4-M3-OA6	82.5(1)	83.6(1)	83.0(1)	83.2(2)
OB1-M3-OA6	75.7(1)	75.4(1)	75.5(1)	75.5(2)
OA3-M3-OA6	98.2(1)	98.4(1)	98.4(1)	98.2(2)
OC4-M3-OA6	65.6(1)	66.2(1)	66.0(1)	65.8(2)
OB4-M4-OB1	110.9(1)	113.1(1)	112.4(2)	112.8(2)
OB4-M4-OA1	102.3(1)	101.9(1)	102.1(2)	102.1(2)
OB1-M4-OA1	118.3(1)	117.0(1)	117.9(2)	117.6(2)
OB1-M4-OA6	82.9(1)	82.0(1)	82.3(2)	81.9(2)
OA1-M4-OA6	87.6(1)	87.5(1)	87.4(2)	87.4(2)
OB4-M4-OC5	90.4(1)	90.7(1)	90.2(2)	90.5(2)
OB1-M4-OC5	90.2(1)	90.0(1)	90.0(2)	89.8(2)
OA6-M4-OC5	68.6(1)	68.6(1)	68.7(1)	68.5(2)
OB4-M4-OA5	79.3(1)	78.0(1)	78.0(2)	78.2(2)
OA1-M4-OA5	74.9(1)	75.2(1)	75.1(1)	75.0(2)
OA6-M4-OA5	81.6(1)	82.1(1)	82.1(1)	82.0(2)
OC5-M4-OA5	71.2(1)	72.0(1)	71.5(1)	71.7(2)
OB1-Si1-OA1	109.8(1)	109.0(2)	109.1(2)	109.9(3)
OB1-Si1-OC5	114.8(1)	115.1(2)	114.6(2)	114.7(3)
OA1-Si1-OC5	108.2(1)	108.3(2)	108.6(2)	108.3(3)
OB1-Si1-OC1	107.1(1)	107.3(2)	107.4(2)	106.7(3)
OA1-Si1-OC1	112.2(1)	112.4(2)	112.3(2)	112.4(3)
OC5-Si1-OC1	104.7(1)	104.8(2)	104.8(2)	104.9(3)
OB2-Si2-OA2	116.8(1)	116.7(2)	116.7(2)	116.6(3)
OB2-Si2-OC2	110.6(1)	110.2(2)	110.1(2)	109.8(3)
OA2-Si2-OC2	110.2(1)	109.8(2)	110.1(2)	110.3(3)
OB2-Si2-OC1	109.1(1)	109.2(2)	109.3(2)	109.0(3)
OA2-Si2-OC1	107.5(1)	107.1(2)	107.1(2)	107.2(3)
OC2-Si2-OC1	101.6(1)	102.9(2)	102.5(2)	103.0(3)
OB3-Si3-OA3	118.7(1)	118.3(2)	118.3(2)	118.5(3)
OB3-Si3-OC3	109.9(1)	109.3(2)	109.6(2)	109.8(3)
OA3-Si3-OC3	109.6(1)	109.5(2)	109.5(2)	109.4(3)
OB3-Si3-OC2	104.1(2)	104.5(2)	104.4(2)	104.3(4)
OA3-Si3-OC2	110.8(1)	110.7(2)	110.8(2)	110.4(3)
OC3-Si3-OC2	102.5(1)	103.5(2)	103.0(2)	103.5(3)
OB4-Si4-OA4	116.8(1)	116.4(2)	116.7(2)	116.5(3)
OB4-Si4-OC3	100.6(1)	100.7(2)	100.6(2)	100.6(3)
OA4-Si4-OC3	114.9(1)	115.5(2)	115.4(2)	115.1(3)
OB4-Si4-OC4	112.4(1)	112.6(2)	112.3(2)	112.8(3)
OA4-Si4-OC4	107.3(1)	106.8(2)	106.8(2)	107.1(3)
OC3-Si4-OC4	104.2(1)	104.4(2)	104.5(2)	104.3(3)
OA5-Si5-OA6	121.7(1)	121.0(2)	121.0(2)	121.2(3)
OA5-Si5-OC4	112.8(1)	113.2(2)	113.1(2)	113.0(3)
OA6-Si5-OC4	100.9(1)	101.8(2)	101.3(2)	101.0(3)
OA5-Si5-OC5	111.0(1)	110.7(2)	111.4(2)	111.1(3)
OA6-Si5-OC5	104.7(1)	104.8(2)	104.6(2)	105.0(3)
OC4-Si5-OC5	103.9(1)	103.5(2)	103.6(2)	103.9(3)

TABLE 8. — *Continued*

Specimen:	15-4030	15-4031	15-4033	15-4034
OA6-M1-OA1	92.2(1)	92.3 (1)	92.2(1)	92.2(1)
OA5-M1-OA1	91.5(1)	91.1 (1)	91.4(1)	91.3(1)
OA6-M1-OA4	85.8(1)	86.1 (1)	86.0(1)	86.1(1)
OA5-M1-OA4	91.0(1)	91.1 (1)	91.0(1)	91.0(1)
OA6-M1-OA2	103.6(1)	103.7 (1)	103.9(1)	103.9(1)
OA5-M1-OA2	85.3(1)	85.0 (1)	84.8(1)	84.7(1)
OA1-M1-OA2	95.1(1)	95.3 (1)	95.3(1)	94.9(1)
OA4-M1-OA2	81.9(1)	81.9 (1)	81.5(1)	81.8(1)
OA6-M1-OA1	84.0(1)	84.1 (1)	84.2(1)	84.3(1)
OA5-M1-OA1	87.5(1)	87.6 (1)	87.6(1)	87.6(1)
OA1-M1-OA1	80.1(1)	79.7 (1)	79.0(1)	79.2(1)
OA4-M1-OA1	103.3(1)	103.5 (1)	104.5(1)	104.5(1)
OB3-M2-OB2	97.7(1)	98.0 (1)	98.1(1)	98.5(1)
OB3-M2-OA2	84.9(1)	83.9 (1)	83.1(1)	82.5(1)
OB2-M2-OA2	99.6(1)	100.1 (1)	100.6(1)	100.7(1)
OB3-M2-OA3	98.8(1)	99.7 (1)	100.5(1)	101.0(1)
OB2-M2-OA3	82.5(1)	82.3 (1)	81.8(1)	81.7(1)
OB2-M2-OA3	97.0(1)	96.6 (1)	96.5(1)	96.2(1)
OA2-M2-OA3	91.7(1)	91.7 (1)	91.9(1)	92.0(1)
OA3-M2-OA3	84.1(1)	84.1 (1)	83.9(1)	84.0(1)
OB3-M2-OA4	88.4(1)	88.5 (1)	88.5(1)	88.4(1)
OA2-M2-OA4	81.2(1)	80.9 (1)	80.9(1)	81.0(1)
OA3-M2-OA4	96.3(1)	96.3 (1)	96.3(1)	96.2(1)
OA3-M2-OA4	76.9(1)	76.9 (1)	77.0(1)	77.0(1)
OB2-M3-OA4	96.4(1)	96.0 (1)	96.0(1)	95.7(1)
OB2-M3-OB1	102.9(1)	103.1 (1)	103.2(1)	103.4(1)
OA4-M3-OB1	97.6(1)	97.5 (1)	97.6(1)	97.2(1)
OB2-M3-OA3	83.3(1)	83.2 (1)	83.1(1)	82.9(1)
OA4-M3-OA3	82.0(1)	81.9 (1)	81.8(1)	82.3(1)
OB2-M3-OC4	115.7(1)	115.6 (1)	115.3(1)	115.3(1)
OB1-M3-OC4	81.6(1)	81.9 (1)	81.7(1)	81.6(1)
OA3-M3-OC4	95.3(1)	95.3 (1)	95.6(1)	95.5(1)
OA4-M3-OA6	82.5(1)	82.7 (1)	82.8(1)	83.1(1)
OB1-M3-OA6	75.7(1)	75.6 (1)	75.4(1)	75.1(1)
OA3-M3-OA6	98.0(1)	98.1 (1)	98.4(1)	98.7(1)
OC4-M3-OA6	65.6(1)	65.9 (1)	66.1(1)	66.1(1)
OB4-M4-OB1	110.2(1)	111.1 (1)	112.5(1)	113.2(1)
OB4-M4-OA1	101.8(1)	101.9 (1)	102.5(1)	102.3(1)
OB1-M4-OA1	118.0(1)	117.9 (1)	118.4(1)	118.1(1)
OB1-M4-OA6	83.0(1)	82.7 (1)	82.2(1)	81.9(1)
OA1-M4-OA6	88.0(1)	87.7 (1)	87.2(1)	87.4(1)
OB4-M4-OC5	91.0(1)	90.8 (1)	89.9(1)	89.8(1)
OB1-M4-OC5	90.4(1)	90.2 (1)	89.8(1)	89.8(1)
OA6-M4-OC5	68.7(1)	68.7 (1)	68.6(1)	68.5(1)
OB4-M4-OA5	80.0(1)	79.3 (1)	78.3(1)	77.8(1)
OA1-M4-OA5	75.1(1)	75.1 (1)	74.4(1)	74.6(1)
OA6-M4-OA5	81.8(1)	81.9 (1)	81.7(1)	81.8(1)
OC5-M4-OA5	71.3(1)	71.5 (1)	71.4(1)	71.5(1)
OB1-Si1-OA1	109.9(2)	109.8 (2)	109.4(2)	109.3(2)
OB1-Si1-OC5	114.8(2)	114.9 (2)	114.8(2)	114.7(2)
OA1-Si1-OC5	108.4(2)	108.4 (2)	108.1(2)	108.1(2)
OB1-Si1-OC1	107.1(2)	107.3 (2)	107.1(2)	107.4(2)
OA1-Si1-OC1	112.2(2)	112.0 (2)	112.5(2)	112.6(2)
OC5-Si1-OC1	104.6(2)	104.5 (2)	104.9(2)	104.8(2)
OB2-Si2-OA2	116.7(2)	116.7 (2)	116.8(2)	116.6(2)
OB2-Si2-OC2	110.4(2)	110.6 (2)	110.0(2)	110.0(2)
OA2-Si2-OC2	110.5(2)	110.2 (2)	110.1(2)	110.1(2)
OB2-Si2-OC1	109.1(2)	109.2 (2)	109.3(2)	109.4(2)
OA2-Si2-OC1	107.5(2)	107.2 (2)	107.3(2)	107.1(2)
OC2-Si2-OC1	101.7(2)	101.9 (2)	102.5(2)	102.6(2)
OB3-Si3-OA3	118.4(2)	118.6 (2)	118.4(2)	118.4(2)
OB3-Si3-OC3	110.0(2)	109.7 (2)	109.6(2)	109.2(2)
OA3-Si3-OC3	109.8(2)	109.6 (2)	109.8(2)	109.4(2)
OB3-Si3-OC2	104.1(2)	104.0 (2)	104.4(2)	104.5(2)
OA3-Si3-OC2	110.9(2)	111.0 (2)	110.6(2)	110.9(2)
OC3-Si3-OC2	102.4(2)	102.7 (2)	103.0(2)	103.4(2)
OB4-Si4-OA4	116.2(2)	116.5 (2)	116.6(2)	116.6(2)
OB4-Si4-OC3	100.8(2)	100.6 (2)	100.7(2)	100.9(2)
OA4-Si4-OC3	115.1(2)	115.3 (2)	115.2(2)	115.3(2)
OB4-Si4-OC4	112.7(2)	112.7 (2)	112.5(2)	112.6(2)
OA4-Si4-OC4	107.1(2)	107.0 (2)	107.1(2)	106.8(2)
OC3-Si4-OC4	104.5(2)	104.2 (2)	104.2(2)	104.1(2)
OA5-Si5-OA6	121.8(2)	121.2 (2)	121.6(2)	121.4(2)
OA5-Si5-OC4	112.7(2)	113.1 (2)	112.8(2)	112.8(2)
OA6-Si5-OC4	101.3(2)	101.2 (2)	101.1(2)	101.1(2)
OA5-Si5-OC5	111.0(2)	111.1 (2)	110.9(2)	110.8(2)
OA6-Si5-OC5	104.5(2)	104.8 (2)	104.9(2)	105.0(2)
OC4-Si5-OC5	103.7(2)	103.7 (2)	103.9(2)	103.9(2)

TABLE 8. — *Continued*

Specimen	15-4006	15-4014	15-4020	15-4027
OA6-M1-OA1	92.44(7)	92.37(6)	92.40(10)	92.5(1)
OA5-M1-OA1	92.34(7)	92.43(7)	92.32(10)	91.9(1)
OA6-M1-OA4	85.72(7)	85.65(6)	85.76(9)	85.9(1)
OA5-M1-OA4	90.14(7)	90.19(6)	90.13(10)	90.4(1)
OA6-M1-OA2	104.37(7)	104.23(6)	104.30(10)	104.4(1)
OA5-M1-OA2	85.09(7)	85.31(6)	85.07(10)	85.1(1)
OA1-M1-OA2	94.84(6)	94.95(6)	94.97(9)	94.7(1)
OA4-M1-OA2	81.96(6)	81.86(6)	81.91(9)	82.2(1)
OA6-M1-OA1	82.05(7)	81.96(6)	82.02(9)	82.2(1)
OA5-M1-OA1	88.93(6)	88.93(6)	89.04(9)	88.7(1)
OA1-M1-OA1	80.89(7)	80.89(7)	80.78(10)	80.8(1)
OA4-M1-OA1	102.60(7)	102.58(6)	102.60(9)	102.6(1)
OB3-M2-OB2	97.63(7)	97.13(7)	97.66(10)	98.0(1)
OB3-M2-OA2	85.35(7)	86.17(7)	85.30(10)	84.4(1)
OB2-M2-OA2	99.43(7)	98.74(7)	99.23(10)	99.7(1)
OB3-M2-OA3	98.43(7)	97.72(7)	98.47(10)	99.2(1)
OB2-M2-OA3	82.43(7)	82.88(6)	82.46(10)	82.3(1)
OB2-M2-OA3	96.03(7)	96.50(6)	95.99(9)	95.8(1)
OA2-M2-OA3	91.95(6)	91.86(6)	91.94(9)	91.9(1)
OA3-M2-OA3	83.83(7)	83.87(6)	83.89(10)	84.0(1)
OB3-M2-OA4	88.99(7)	89.07(7)	89.00(10)	89.0(1)
OA2-M2-OA4	81.58(6)	81.69(6)	81.60(9)	81.6(1)
OA3-M2-OA4	77.35(6)	77.30(6)	77.36(9)	95.9(1)
OA3-M2-OA4	96.12(6)	96.26(6)	96.26(9)	77.3(1)
OB2-M3-OA4	95.99(7)	96.27(7)	95.88(10)	95.6(1)
OB2-M3-OB1	102.99(7)	102.81(7)	102.98(10)	103.0(1)
OA4-M3-OB1	96.24(7)	96.45(7)	96.15(10)	96.1(1)
OB2-M3-OA3	83.72(7)	83.84(7)	83.64(10)	83.5(1)
OA4-M3-OA3	82.26(7)	81.91(7)	82.35(10)	82.1(1)
OB2-M3-OC4	116.17(7)	116.30(7)	116.33(10)	116.0(1)
OB1-M3-OC4	81.97(7)	82.08(7)	82.02(10)	82.6(1)
OA3-M3-OC4	95.74(7)	95.74(6)	95.72(10)	95.6(1)
OA4-M3-OA6	82.56(6)	82.38(6)	82.51(9)	82.7(1)
OB1-M3-OA6	74.27(7)	74.52(6)	74.35(9)	74.5(1)
OA3-M3-OA6	99.01(7)	98.81(6)	99.00(9)	99.0(1)
OC4-M3-OA6	65.58(6)	65.37(6)	65.57(9)	66.0(1)
OB4-M4-OB1	112.86(8)	112.25(7)	113.02(11)	113.1(1)
OB4-M4-OA1	102.98(8)	102.90(7)	103.01(11	)102.8(1)
OB1-M4-OA1	119.91(8)	120.15(7)	120.03(11)	119.4(1)
OB1-M4-OA6	83.90(7)	84.13(7)	83.94(10)	83.7(1)
OA1-M4-OA6	86.94(7)	87.03(7)	86.84(10)	86.9(1)
OB4-M4-OC5	87.46(7)	87.79(7)	87.37(10)	87.8(1)
OB1-M4-OC5	90.77(7)	90.87(7)	90.71(10)	90.8(1)
OA6-M4-OC5	68.15(6)	68.04(6)	68.09(9)	68.4(1)
OB4-M4-OA5	77.56(7)	78.09(6)	77.37(9)	77.5(1)
OA1-M4-OA5	74.04(7)	73.98(6)	74.00(9)	74.4(1)
OA6-M4-OA5	79.22(7)	79.16(6)	79.17(9)	79.5(1)
OC5-M4-OA5	69.30(7)	69.14(5)	69.24(8)	69.5(1)
OB1-Si1-OA1	109.3(1)	109.38(10)	109.3(1)	109.2(2)
OB1-Si1-OC5	114.5(1)	114.42(10)	114.5(1)	114.9(2)
OA1-Si1-OC5	109.0(1)	109.09(10)	109.0(1)	109.0(2)
OB1-Si1-OC1	107.6(1)	107.31(10)	107.4(1)	107.3(2)
OA1-Si1-OC1	111.9(1)	111.68(9)	111.9(1)	111.7(2)
OC5-Si1-OC1	104.6(1)	104.93(9)	104.8(1)	104.6(2)
OB2-Si2-OA2	117.0(1)	116.98(9)	116.9(1)	116.8(2)
OB2-Si2-OC2	110.7(1)	110.77(10)	110.8(1)	110.4(2)
OA2-Si2-OC2	110.3(1)	110.22(9)	110.0(1)	110.3(2)
OB2-Si2-OC1	108.6(1)	108.67(9)	108.8(1)	108.9(2)
OA2-Si2-OC1	107.5(1)	107.58(9)	107.6(1)	107.3(2)
OC2-Si2-OC1	101.6(1)	101.40(9)	101.7(1)	102.1(2)
OB3-Si3-OA3	118.0(1)	118.37(10)	118.2(2)	118.2(2)
OB3-Si3-OC3	110.2(1)	110.29(10)	110.2(1)	110.1(2)
OA3-Si3-OC3	109.9(1)	109.85(9)	109.9(1)	109.6(2)
OB3-Si3-OC2	104.4(1)	104.11(10)	104.4(2)	104.3(2)
OA3-Si3-OC2	110.8(1)	110.83(9)	110.7(1)	110.8(2)
OC3-Si3-OC2	102.2(1)	102.03(9)	102.2(1)	102.5(2)
OB4-Si4-OA4	117.0(1)	116.91(10)	116.9(1)	116.8(2)
OB4-Si4-OC3	100.4(1)	100.52(9)	100.4(1)	100.8(2)
OA4-Si4-OC3	114.8(1)	114.40(9)	115.0(1)	114.8(2)
OB4-Si4-OC4	112.5(1)	112.52(10)	112.5(2)	112.7(2)
OA4-Si4-OC4	107.4(1)	107.75(9)	107.4(1)	107.2(2)
OC3-Si4-OC4	104.1(1)	104.00(9)	104.0(1)	103.9(2)
OA5-Si5-OA6	121.8(1)	121.71(9)	121.6(1)	121.5(2)
OA5-Si5-OC4	112.3(1)	112.38(9)	112.4(1)	112.8(2)
OA6-Si5-OC4	101.1(1)	101.06(9)	101.0(1)	101.2(2)
OA5-Si5-OC5	110.9(1)	110.96(9)	111.0(1)	110.7(2)
OA6-Si5-OC5	105.3(1)	105.23(9)	105.5(1)	105.3(2)
OC4-Si5-OC5	103.7(1)	103.66(9)	103.7(1)	103.6(2)

TABLE 8. — *Continued*

Specimen	15-4028	15-4029	15-4040	15-4041
OA6-M1-OA1	92.37(7)	92.27(6)	92.4(1)	92.39(7)
OA5-M1-OA1	92.41(7)	92.56(6)	92.6(1)	92.55(7)
OA6-M1-OA4	85.69(7)	85.58(6)	85.6(1)	85.52(7)
OA5-M1-OA4	90.15(7)	90.22(6)	90.1(1)	90.19(7)
OA6-M1-OA2	104.12(7)	104.07(6)	104.2(1)	85.43(7)
OA5-M1-OA2	85.21(7)	85.35(6)	85.1(1)	104.19(7)
OA1-M1-OA2	95.12(6)	95.02(6)	94.9(1)	94.97(7)
OA4-M1-OA2	81.74(6)	81.84(6)	82.0(1)	81.88(7)
OA6-M1-OA1	82.39(7)	82.39(6)	82.3(1)	82.23(7)
OA5-M1-OA1	88.73(6)	88.62(6)	88.9(1)	88.60(7)
OA1-M1-OA1	80.49(7)	80.76(7)	80.8(1)	80.73(7)
OA4-M1-OA1	102.94(6)	102.69(6)	102.7(1)	102.72(7)
OB3-M2-OB2	97.16(7)	96.97(7)	97.1(1)	97.00(7)
OB3-M2-OA2	85.82(7)	86.29(7)	85.9(1)	86.30(7)
OB2-M2-OA2	99.08(7)	98.58(6)	98.8(1)	98.37(7)
OB3-M2-OA3	96.63(7)	97.60(7)	97.8(1)	97.54(7)
OB2-M2-OA3	98.05(7)	96.75(6)	96.5(1)	83.16(7)
OB2-M2-OA3	82.69(7)	82.93(6)	82.9(1)	96.70(7)
OA2-M2-OA3	91.88(7)	91.94(6)	91.9(1)	91.89(7)
OA3-M2-OA3	83.83(7)	83.82(6)	84.0(1)	83.92(7)
OB3-M2-OA4	88.94(7)	88.98(6)	89.0(1)	89.03(7)
OA2-M2-OA4	81.53(6)	81.66(6)	81.7(1)	81.77(7)
OA3-M2-OA4	77.27(6)	77.30(6)	77.4(1)	77.27(7)
OA3-M2-OA4	96.27(6)	96.42(6)	96.2(1)	96.28(7)
OB2-M3-OA4	96.34(7)	96.49(7)	96.4(1)	96.27(7)
OB2-M3-OB1	102.84(7)	102.90(7)	102.7(1)	102.82(7)
OA4-M3-OB1	96.74(7)	96.52(7)	96.3(1)	96.57(7)
OB2-M3-OA3	83.68(7)	83.76(6)	83.9(1)	83.75(7)
OA4-M3-OA3	81.77(7)	81.65(6)	82.0(1)	81.62(7)
OB2-M3-OC4	116.06(7)	116.45(6)	116.3(1)	116.51(7)
OB1-M3-OC4	82.09(7)	82.13(6)	82.3(1)	82.12(7)
OA3-M3-OC4	95.68(7)	95.80(6)	95.6(1)	95.87(7)
OA4-M3-OA6	82.34(6)	82.04(6)	82.2(1)	82.24(7)
OB1-M3-OA6	74.79(7)	74.76(6)	74.8(1)	74.77(7)
OA3-M3-OA6	98.68(7)	98.56(6)	98.6(1)	98.64(7)
OC4-M3-OA6	65.55(6)	65.30(6)	65.4(1)	65.27(6)
OB4-M4-OB1	112.10(8)	111.97(7)	112.3(1)	111.80(8)
OB4-M4-OA1	102.92(8)	102.78(7)	102.7(1)	102.69(8)
OB1-M4-OA1	119.91(7)	119.99(7)	119.9(1)	120.07(8)
OB1-M4-OA6	83.86(7)	84.00(7)	83.9(1)	84.16(7)
OA1-M4-OA6	86.92(7)	87.06(6)	87.0(1)	87.19(7)
OB4-M4-OC5	88.19(7)	88.16(7)	88.0(1)	88.22(7)
OB1-M4-OC5	90.84(7)	91.02(7)	91.0(1)	91.10(7)
OA6-M4-OC5	68.20(6)	68.18(6)	68.4(1)	68.06(6)
OB4-M4-OA5	78.24(6)	78.41(6)	78.2(1)	78.44(7)
OA1-M4-OA5	74.05(6)	74.00(6)	74.1(1)	73.98(6)
OA6-M4-OA5	79.62(6)	79.44(6)	79.6(1)	79.42(6)
OC5-M4-OA5	69.34(6)	69.18(5)	69.3(1)	69.13(6)
OB1-Si1-OA1	109.5(1)	109.54(9)	109.3(2)	109.4(1)
OB1-Si1-OC5	114.6(1)	114.61(10)	114.5(2)	114.5(1)
OA1-Si1-OC5	108.8(1)	108.81(9)	109.4(2)	109.1(1)
OB1-Si1-OC1	107.4(1)	107.27(9)	107.0(2)	107.4(1)
OA1-Si1-OC1	111.7(1)	111.71(9)	111.8(2)	111.7(1)
OC5-Si1-OC1	104.8(1)	104.86(9)	104.9(1)	104.8(1)
OB2-Si2-OA2	117.0(1)	117.02(9)	116.7(2)	116.9(1)
OB2-Si2-OC2	110.7(1)	110.75(9)	110.7(2)	110.7(1)
OA2-Si2-OC2	110.1(1)	110.26(9)	110.4(2)	110.4(1)
OB2-Si2-OC1	108.8(1)	108.64(9)	108.6(2)	108.7(1)
OA2-Si2-OC1	107.5(1)	107.63(9)	107.8(2)	107.9(1)
OC2-Si2-OC1	101.5(1)	101.31(9)	101.4(1)	101.1(1)
OB3-Si3-OA3	118.4(1)	118.37(9)	118.4(2)	118.4(1)
OB3-Si3-OC3	110.2(1)	110.44(9)	110.1(2)	110.3(1)
OA3-Si3-OC3	109.8(1)	109.79(9)	109.8(2)	109.9(1)
OB3-Si3-OC2	104.2(1)	104.02(9)	104.1(2)	103.9(1)
OA3-Si3-OC2	110.8(1)	110.78(9)	111.0(2)	110.9(1)
OC3-Si3-OC2	102.1(1)	102.09(9)	102.2(1)	102.1(1)
OB4-Si4-OA4	116.8(1)	116.74(9)	116.7(2)	116.7(1)
OB4-Si4-OC3	100.6(1)	100.49(9)	100.5(2)	100.5(1)
OA4-Si4-OC3	114.6(1)	114.64(9)	114.6(2)	114.6(1)
OB4-Si4-OC4	112.5(1)	112.49(9)	112.7(2)	112.4(1)
OA4-Si4-OC4	107.5(1)	107.63(9)	107.6(2)	107.7(1)
OC3-Si4-OC4	104.2(1)	104.17(9)	104.1(2)	104.2(1)
OA5-Si5-OA6	121.6(1)	121.71(9)	121.6(2)	121.9(1)
OA5-Si5-OC4	112.3(1)	112.25(9)	112.3(2)	112.2(1)
OA6-Si5-OC4	101.0(1)	100.95(9)	100.9(2)	101.0(1)
OA5-Si5-OC5	111.1(1)	111.00(9)	111.5(2)	111.0(1)
OA6-Si5-OC5	105.2(1)	105.21(9)	105.0(2)	105.2(1)
OC4-Si5-OC5	103.8(1)	103.93(9)	103.7(2)	103.7(1)

was distributed equally among all five M sites to avoid biasing the results, inasmuch as Fe has the highest electronegativity of all the cations involved. The assumptions inherent in this cation-assignment procedure may cause some of the scatter seen in Figure 8, but it is nevertheless clear that a strong correlation exists between the electron population and electronegativity. Given the well known relationship between covalency and difference in electronegativity (Pauling 1960), Figures 5 through 8 imply an increase in the covalency of the M4 site with increasing tetrahedral character. The shift from fivefold coordination in Mg-rich and typical Mn-rich rhodonite toward tetrahedral coordination in fowlerite may thus be related to a preference of Zn for local increased covalency.

Turning now to M5, Table 13 displays the simple correlation coefficients between two measures of site geometry (mean bond length and quadratic elongation; Robinson et al. 1971) and three characteristics of the occupying cations (electron population from site refinements, mean electronegativity, and mean seven-coordinated effective ionic radius (Shannon 1976)). Correlation coefficients were determined using all 16 refined specimens. The correlations between mean ionic radius and M5 site geometry have intuitively correct signs: as ionic radius increases, the mean size of M5 generally increases, and quadratic elongation decreases because the larger cation must be located closer to the centroid of the site. Nevertheless, the correlations are not quantitatively impressive. Although these relatively poor correlations might be attributed to inaccuracy in our assignment of cations, the mean electronegativity, which is strongly corre-

TABLE 9. Plausible cation distributions* for typical specimens of fowlerite and rhodonite

	Mn	Fe	Mg	Zn	Ca	Occupancy (atoms)	Electrons (probe)	Electrons (X-ray)
Fowlerite (15-4029)								
M1	0.921	0.041			0.038	1.000	24.85	24.91
M2	0.910	0.041			0.050	1.001	24.82	24.67
M3	0.910	0.041			0.050	1.001	24.82	24.64
M4	0.440	0.041	0.130	0.410		1.021	25.93	26.98
M5	0.094	0.045			0.863	1.002	20.78	20.41
Totals						5.025	121.20	121.61
Rhodonite (15-4024)								
M1	0.871	0.080			0.050	1.001	24.86	24.90
M2	0.871	0.080			0.050	1.001	24.86	24.90
M3	0.824	0.080			0.100	1.004	24.68	24.70
M4	0.822	0.080	0.100	0.005		1.007	23.98	24.30
M5	0.857	0.080			0.100	1.037	25.51	25.90
Totals						5.051	123.89	124.70

* From microprobe analysis shown in Table 1, but based on the asymmetric unit (i.e., 15 oxygen atoms instead of 3 oxygen atoms).

TABLE 10. Principle component analysis for (a) rhodonites and (b) fowlerites in this study

(a) rhodonites Rotated factor pattern			(b) fowlerites Rotated factor pattern		
Mn	–0.087	–0.996	Mn	–0.033	0.965
Fe	–0.506	0.861	Fe	0.170	–0.894
Mg	0.942	–0.145	Mg	0.987	–0.039
Ca	0.963	–0.048	Zn	0.854	–0.376
			Ca	–0.949	0.011
Variance	2.08	1.76	Variance	2.63	1.87
% of total	52	44	% of total	53	37

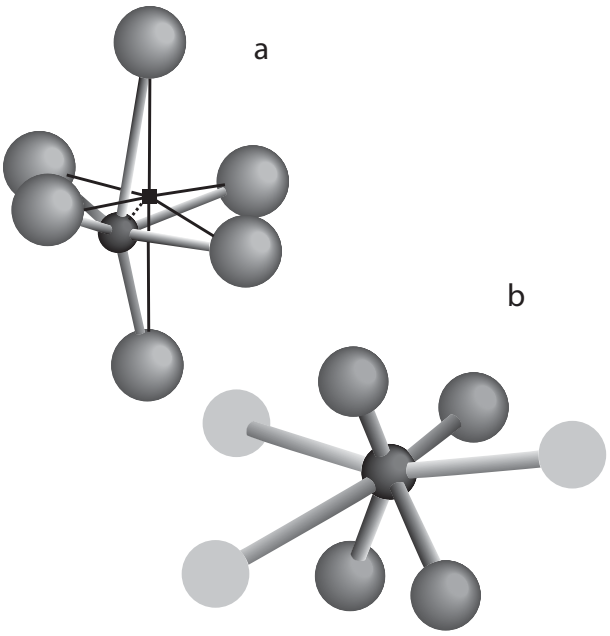

FIGURE 6. (**a**) Displacement of the cation from the centroid of the M4 site, considered as an octahedron. (**b**) M4 coordination sphere with the three longest distances subdued, showing the tetrahedral disposition of the four shortest bonds.

TABLE 11. Mean M-O bond lengths from structure refinements

	15-4018	15-4024	15-4025	15-4026	15-4030	15-4031	15-4033	15-4034
<M1-O>	2.222	2.216	2.218	2.216	2.225	2.218	2.209	2.210
<M2-O>	2.221	2.232	2.228	2.224	2.223	2.222	2.218	2.221
<M3-O>	2.224	2.218	2.223	2.216	2.228	2.223	2.216	2.213
<M4-O>[6]	2.266	2.261	2.265	2.262	2.265	2.258	2.263	2.261
<M4-O>[5]	2.144	2.149	2.149	2.146	2.145	2.141	2.143	2.143
<M4-O>[4]	2.087	2.096	2.095	2.093	2.090	2.086	2.087	2.085
<M5-O>[7]	2.416	2.397	2.402	2.404	2.420	2.408	2.402	2.396
<M5-O>[6]	2.376	2.333	2.345	2.348	2.383	2.362	2.348	2.337
	15-4006	15-4014	15-4020	15-4027	15-4028	15-4029	15-4040	15-4041
<M1-O>	2.218	2.225	2.217	2.218	2.222	2.224	2.224	2.228
<M2-O>	2.216	2.217	2.214	2.221	2.216	2.216	2.219	2.219
<M3-O>	2.219	2.226	2.219	2.218	2.225	2.229	2.225	2.233
<M4-O>[6]	2.259	2.266	2.260	2.257	2.267	2.270	2.269	2.271
<M4-O>[5]	2.117	2.123	2.117	2.119	2.128	2.129	2.127	2.129
<M4-O>[4]	2.039	2.045	2.038	2.043	2.054	2.054	2.053	2.054
<M5-O>[7]	2.413	2.424	2.411	2.410	2.422	2.427	2.422	2.428
<M5-O>[6]	2.373	2.392	2.372	2.363	2.387	2.397	2.389	2.399

Note: Numbers in square brackets are coordination numbers.

TABLE 12. Correlations between mean bond lengths and unit-cell parameters

	a	*b*	*c*	α	β	γ
(a) rhodonite specimens						
<M1-O>	0.87	0.94	0.48	0.08	0.31	–0.20
<M2-O>	–0.20	0.06	–0.08	–0.83	–0.77	0.82
<M3-O>	0.91	0.89	0.60	0.12	0.49	–0.35
<M4-O>	–0.18	0.09	0.25	–0.74	–0.58	0.59
<M5-O>	0.98	0.92	0.58	0.57	0.76	–0.68
	a	*b*	*c*	α	β	γ
(b) fowlerite specimens						
<M1-O>	0.96	0.97	0.94	0.37	0.50	–0.66
<M2-O>	0.24	0.39	0.30	–0.45	–0.45	0.25
<M3-O>	0.98	0.98	0.97	0.48	0.63	–0.76
<M4-O>	0.89	0.95	0.96	0.33	0.40	–0.68
<M5-O>	0.99	0.96	0.98	0.53	0.67	–0.84

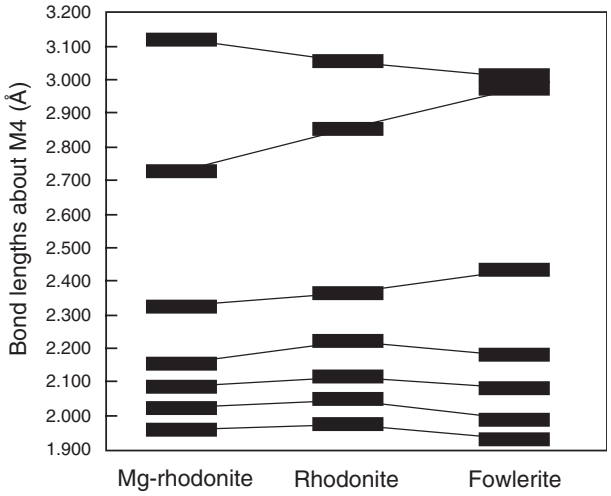

FIGURE 7. Trends in M4 bond lengths. The bars represent average values of the bond lengths. The bars labeled Mg-rich rhodonite are averages of data from Peacor et al. (1978) and Murakami and Takéuchi (1979). All other specimens used are from this study. The large size of Mn results in the four shortest bonds about M4 of rhodonite being slightly longer than their counterparts in Mg-rich or Zn-rich rhodonite.

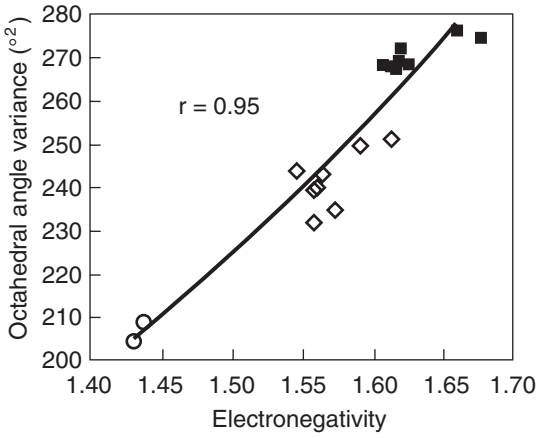

FIGURE 8. Octahedral angle variance (σ_o^2) at M4 as a function of electronegativity calculated using X-ray site refinements and microprobe analyses.

lated with site geometry, is dependent on the same assignment. Stepwise multiple linear regression confirms that, pitted against electron population or mean electronegativity, mean ionic radius is, at best, marginally significant as a predictor of either the size or distortion of M5.

Figure 9 displays quadratic elongation for M5 as a function of electron population from X-ray site refinements (Table 5). The trend indicates that the bond lengths become more uniform as the number of electrons decreases (i.e., as Ca concentration increases). Some overlap occurs between the ranges for fowlerite and rhodonite specimens. The rhodonite specimens in the overlap region have large Ca contents. The two specimens at opposite ends of the trend are 15-4024 (rhodonite, large quadratic elongation) and 15-4041 (fowlerite, small quadratic elongation). Comparison of bond lengths (Table 7) shows that the range for M5 is twice as large in 15-4024 as in 15-4041 (2.175-2.780 and 2.305-2.604 Å, respectively), although the average M5-O distance is slightly larger for fowlerite than for rhodonite (Table 11). Because the electronegativity of Ca is smaller than that of any other cation in the M sites, increased Ca concentration inevitably leads to increased ionicity. It appears that as M4 becomes more Zn-rich, tetrahedral, and covalent in character, M5 becomes more Ca-rich, less distorted, and more ionic in character.

ACKNOWLEDGMENTS

D. Peacor (University of Michigan) and an anonymous referee made comments and suggestions that were helpful in improving the manuscript. We also benefited from a discussion with B. Campbell (BYU). We are also grateful for an undergraduate mentorship granted to the senior author by the College of Physical and Mathematical Sciences, BYU, which provided partial financial support.

REFERENCES CITED

Abrahams, S.C. and Bernstein, J.L. (1969) Remeasurement of the structure of hexagonal ZnO. Acta Crystallographica, B25, 1233–1236.
Allred, A.L. (1961) Electronegativity values from thermochemical data. Journal

TABLE 13. Correlations between M5 geometry and mean cation characteristics

	Electron population (e^-)	<Electronegativity>	$<^{[7]}$Ionic radius> (Å)
$<^{[7]}$M5-O> (Å)	–0.9477	–0.8747	0.6330
Quadratic elongation (Å²)	0.9633	0.8868	–0.5650

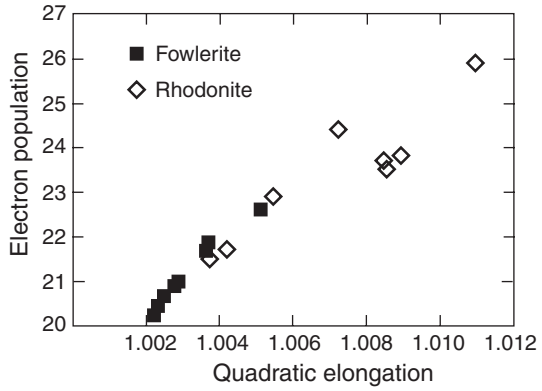

FIGURE 9. Quadratic elongation vs. electron population for M5 in our specimens.

of Inorganic and Nuclear Chemistry, 17, 215–221.
Bindi, L., Czank, M., Rothlisberger, F., and Bonazzi, P. (2001) Hardystonite from Franklin furnace: A natural modulated melilite. American Mineralogist, 86, 747–751.
Camac, M.D. (1852) Analysis of fowlerite. American Journal of Science, 14, 418–419.
Chao, G.Y. (1969) Refinement of the crystal structure of parahopeite. Zeitschrift für Kristallographie, 130, 261–266.
Cromer, D.T. and Mann, J.B. (1968) X-ray scattering factors computed from numerical Hartree-Fock wave functions. Acta Crystallographica, A24, 321–324.
Dickson, B.L. (1975) The iron distribution in rhodonite. American Mineralogist, 60, 98–104.
Evans, R.C. (1966) An Introduction to Crystal Chemistry, 411 p. University Press, Cambridge.
Farrugia, L.J. (1999) WinGX suite for small-molecule single-crystal crystallography. Journal of Applied Crystallography, 32, 837–838.
Fehr, K.T. (2001) Stability and phase relations of $Ca[ZnSi_3]O_8$, a new phase with feldspar structure in the system CaO-ZnO-SiO_2. American Mineralogist, 86, 21–28.
Ghose, S., Leo, S.R., and Wan, C. (1974) Structural chemistry of copper and zinc minerals. Part I. Veszelyite, $(Cu,Zn)_2ZnPO_4(OH)_3 \cdot 2H_2O$: A novel type of sheet structure and crystal chemistry of copper-zinc substitution. American Mineralogist, 59, 573–581.
Griffen, D.T. (1981) Synthetic Fe/Zn staurolites and the ionic radius of $^{IV}Zn^{2+}$. American Mineralogist, 66, 932–937.
Griffen, D.T. and Ribbe, P.H. (1973) The crystal chemistry of staurolite. American Journal of Science, 273-A, 479–495.
Ito, J. (1972) Rhodonite-pyroxmangite peritectic along the join $MnSiO_3$-$MgSiO_3$ in air. American Mineralogist, 57, 865–876.
Libowitzky, E., Schultz, A.J., and Young, D.M. (1998) The low-temperature structure and phase transition of hemimorphite, $Zn_4Si_2O_7(OH) \cdot H_2O$. Zeitschrift für Kristallographie, 213, 659–668.
Liebau, F. (1959) Über die Kristallstruktur des Pyroxmangits $(Mn,Fe,Ca,Mg)SiO_3$. Acta Crystallographica, 12, 177–181.
Liebau, F., Hilmer, W., and Lindemann, G. (1959) Über die Kristallstruktur des Rhononit $(Mn,Ca)SiO_3$. Acta Crystallographica, 12, 182–187.
Livi, K.J.T. and Veblen, D.R. (1992) An analytical electron microscopy study of pyroxene-to-pyroxenoid reactions. American Mineralogist, 77, 380–390.
Louisnathan, S.J. (1969) Refinement of the crystal structure of hardystonite, $Ca_2ZnSi_2O_7$. Zeitschrift für Kristallographie, 130, 427–437
Lucchesi, S., Russo, U., and Della Giusta, A. (1999) Cation distribution in natural Zn-spinels: franklinite. European Journal of Mineralogy, 11, 501–511.
Mihaljevic, M. (1999) Zinc. In C.P. Marshall and R.W. Fairbridge, Eds., Encyclopedia of Geochemistry, p. 674–675. Kluwer, Dordrecht.
Momoi, H. (1964) Mineralogical study of rhodonites in Japan, with special reference to contact metamorphism. Memoirs of the Faculty of Science, Kyushu University, 15, 39–63.
Murakami, T. and Takéuchi, Y. (1979) Structure of synthetic rhodonite, $Mn_{0.685}Mg_{0.315}SiO_3$, and compositional transformations in pyroxenoids. Mineralogical Journal, 9, 286–304.
North, A.C.T., Phillips, D.C., and Mathews, F.S. (1968) A semi-empirical method of absorption correction. Acta Crystallographica, A24, 351–359.
Ohashi, Y. and Finger, L.W. (1975) Pyroxenoids: A comparison of refined structures of rhodonite and pyroxmangite. Carnegie Institute Washington Year Book, 74, 564–569.
O'Neill, H.St.C. and Dollase, W.A. (1994) Crystal structures and cation distributions in simple spinels from powder XRD structural refinements: $MgCr_2O_4$, $ZnCr_2O_4$, Fe_3O_4 and the temperature dependence of the cation distribution in $ZnAl_2O_4$. Physics and Chemistry of Minerals, 20, 541–555.
Pauling, L. (1960) The Nature of the Chemical Bond and the Structure of Molecules and Crystals, ed. 3, 644 p. Cornell University Press, Ithaca.
Peacor, D.R. and Niizeki, N. (1963) The redetermination and refinement of the crystal structure of rhodonite $(Mn,Ca)SiO_3$. Zeitschrift für Kristallographie, 119, 98–116.
Peacor, D.R., Essene, E.J., Brown, P.E., and Winter, G.A. (1978) The crystal chemistry and petrogenesis of a magnesian rhodonite. American Mineralogist, 63, 1137–1142
Pinckney, L.R. and Burnham, C.W. (1988) Effects of compositional variation on the crystal structures of pyroxmangite and rhodonite. American Mineralogist, 73, 798–808.
Pouchou, J.L. and Pichoir, F. (1985) "PAP" (phi-rho-z) procedure for improved quantitative microanalysis. In J.T. Armstrong, Ed., Microbeam Analysis, pp. 104–106. San Francisco, San Francisco Press.
Rao, C.R. (1965) Linear Statistical Inference and Its Applications, 522 p. Wiley, New York.
Roberts, W.L., Campbell, T.J., and Rapp, G.R. (1992) Encyclopedia of Minerals, ed. 2, 979 p. Van Nostrand Reinhold, New York.
Robinson, K., Gibbs, G.V., and Ribbe, P.H. (1971) Quadratic elongation: A quantitative measure of distortion in coordination polyhedra. Science, 172, 567–570.
Sapountzis, E.A. and Christofides, G. (1982) A calcium-poor rhodonite from Xanthi (N. Greece). Mineralogical Magazine, 46, 337–340.
Shannon, R.D. (1976) Revised effective ionic radii and systematic studies of interatomic distances in halides and chalcogenides. Acta Crystallographica, A32, 751–767.
Sheldrick, G.M. (1997) SHELX-97, a program for crystal structure refinement. University of Göttingen, Germany.
Shepard, C.U. (1832) Sketch of the mineralogy and geology of the counties of Orange, N.Y., and Sussex, N.J. American Journal of Science, 21, 321–334.
Smyth, J.R., Jacobsen, S.D., and Hazen, R.M. (2000) Comparative crystal chemistry of dense oxide minerals. In R.M. Hazen and R.T. Downs, Eds., High-Temperature and High-Pressure Crystal Chemistry. Reviews in Mineralogy and Geochemistry, 41, 157–186. Mineralogical Society of America, Washington, D.C.
Torrey, J. (1822) Mineralogical Notices. American Journal of Science, 5, 399–403.
Viswanathan, K. and Harneit, O. (1986) Lattice expansion and ionic substitution in common pyroxenoids. Contributions to Mineralogy and Petrology, 94, 238–244.

MANUSCRIPT RECEIVED APRIL 29, 2004
MANUSCRIPT ACCEPTED OCTOBER 16, 2004
MANUSCRIPT HANDLED BY MARIA BRIGATTI